Volume 8 | Number 8 | 21 April 2024

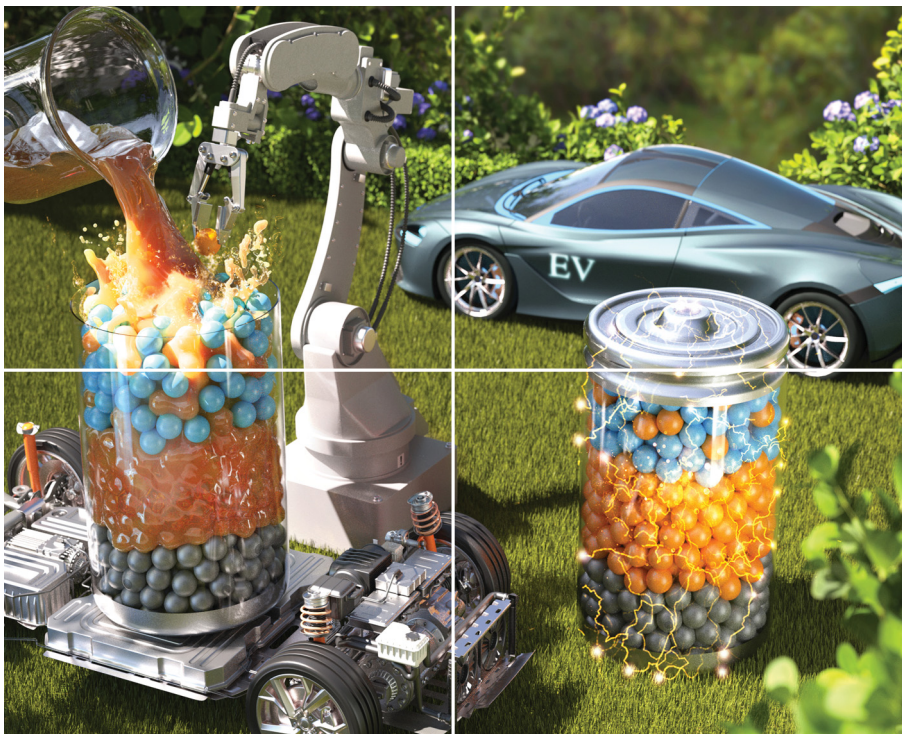

MATERIALS CHEMISTRY

FRONTIERS

CCS 中国化学会 CHINESE CHEMICAL SOCIETY
ICCAS 1956
ROYAL SOCIETY OF CHEMISTRY
rsc.li/frontiers-materials

MATERIALS CHEMISTRY
FRONTIERS

REVIEW

View Article Online
View Journal | View Issue

Cite this: *Mater. Chem. Front.*, 2024, **8**, 1861

Recent advances in all-solid-state batteries for commercialization

Junghwan Sung,[ab] Junyoung Heo,[ab] Dong-Hee Kim,[a] Seongho Jo,[d] Yoon-Cheol Ha,[ab] Doohun Kim,[ab] Seongki Ahn*[c] and Jun-Woo Park*[ab]

All-solid-state batteries (ASSB) have gained significant attention as next-generation battery systems owing to their potential for overcoming the limitations of conventional lithium-ion batteries (LIB) in terms of stability and high energy density. This review presents progress in ASSB research for practical applications. It focuses on membrane production strategies, highlighting the need for considerations such as productivity, cost-effectiveness, and eco-friendliness. Various fabrication techniques aimed at achieving enhanced safety and energy density are introduced. Additionally, this review introduces efforts towards the commercialization of ASSB electrode manufacturing and emerging research trends in the field. We highlight the challenges and advancements in these areas and discuss the prospects of ASSBs as practical alternatives to LIBs for various applications. This review is valuable for researchers and industry professionals seeking guidance in facilitating ASSB commercialization.

Received 1st November 2023,
Accepted 8th January 2024

DOI: 10.1039/d3qm01171b

rsc.li/frontiers-materials

[a] *Battery Research Division, Korea Electrotechnology Research Institute (KERI), 12, Jeongiui-gil, Seongsan-gu, Changwon-si, Gyeongsangnam-do, 51543, Republic of Korea. E-mail: parkjw@keri.re.kr*
[b] *Department of Electro-Functionality Materials Engineering, University of Science and Technology (UST), Daejeon 305-333, Republic of Korea*
[c] *Department of Chemical Engineering, Hankyong National University, 27, Jungangro, Anseong-si, Gyeonggi-do, 17579, Republic of Korea. E-mail: skahn@hknu.ac.kr*
[d] *Department of New Energy and Mining Engineering, Sangji University, 83, Sangjidae-gil, Wonju-si, Gangwon-do, 26339, Republic of Korea*

1. Introduction

1.1. Background

Since their initial release by Sony in 1991, lithium-ion batteries (LIB) have undergone substantial development and are widely utilized as electrochemical energy storage devices.[1–6] LIBs have extensive applications not only in electronic products, but also in various large-scale sectors, including the electric vehicle (EV) industry,[7–11] energy storage system (ESS) market,[12–16] and artificial intelligence (AI) and information technology (IT) industries.[17–25] This rapid increase in demand is expected to make LIBs a dominant force in the automotive industry over the next decade.

Junghwan Sung

Junghwan Sung is currently a PhD degree student at the University of Science and Technology. He received his BS and Master's degrees in Department of Metallurgical Engineering from Pukyong National University. He is affiliated with the Battery Research Division of the Korea Electrotechnology Research Institute (KERI). His research focuses on fabricating electrodes and electrolytes for all-solid-state batteries.

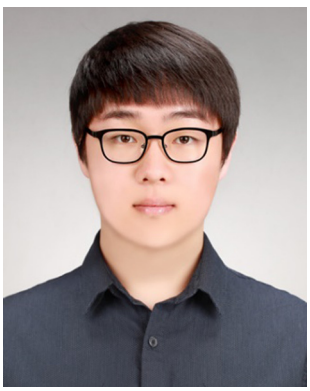

Junyoung Heo

Junyoung Heo is currently a master's degree student at the University of Science and Technology. He received his BS degrees at the Department of Electrical Engineering from Yeungnam University. He is affiliated with the Battery Research Division of the Korea Electrotechnology Research Institute (KERI). His research interests mainly focus on lithium–sulfur batteries, as well as solid-state lithium–sulfur batteries.

Based on survey results from the US DOE Global Energy Storage Database, the installed capacity of LIBs is projected to increase annually.[26] This highlights the importance of developing innovative processes and advancing their commercialization. However, conventional LIBs still face various issues and challenges with enhanced attributes, such as higher energy density, longer lifespan, reduced cost, and improved eco-friendliness, to meet the demands of next-generation LIB markets.[27–30] Despite serving as major energy storage devices for electronic devices owing to their high energy density and rechargeable nature, as technology and society's reliance on electronics has advanced, new challenges have emerged for LIBS.

Although LIBs have been instrumental in powering portable electronics, prominent concerns such as their inherent flammability and potential for thermal runaway, particularly when exposed to high temperatures or physical damage, remain. This has led to incidents and concerns regarding the use of LIBs in applications such as EVs and large-scale ESSs.[31–34] Furthermore, LIBs have certain limitations in terms of their energy density and capacity. The theoretical capacities of various lithium-ion cathode materials are limited to specific ranges (*e.g.*, $LiCoO_2$: 140 mA h g^{-1}, $LiFePO_4$: 170 mA h g^{-1}, $LiMnO_2$: 286 mA h g^{-1}, $LiNiMnCoO_2$: 280 mA h g^{-1}). This means that even with advancements in their design, LIBs are reaching a point where further significant improvements in energy density might be challenging to achieve.[35–37] This underscores their limitations and drives the need for alternative battery technologies.[38–40]

The growing demand for large-scale energy storage solutions, particularly those driven by renewable energy integration and EV adoption, has highlighted the need for batteries with higher energy densities, improved safety, and more sustainable materials. To overcome the challenges associated with LIBs, researchers have been actively exploring various approaches for developing next-generation batteries. These efforts include investigating alternative ion systems such as sodium-ion,[41–45] and magnesium-ion batteries,[46–50] as well as new cathode materials with higher theoretical capacities than conventional nickel- and cobalt-based cathode materials, such as sulfur-based cathodes.[51–55] Additionally, the interest in transitioning from liquid electrolytes to solid-state electrolytes (SSE) to enhance battery performance and safety has grown.[56–60] These advancements aim to address the limitations of the current LIBs and establish more efficient and sustainable energy storage solutions.

1.2. All-solid-state batteries (ASSB)

As an advanced and state-of-the-art next-generation battery technology, ASSBs are being actively developed as promising alternatives to conventional LIBs.[61–63] ASSBs offer numerous advantages, such as electrochemical energy storage and power sources. These advantages include improved safety, enhanced energy density, higher thermal stability, and potentially longer lifespan.[64–67] The use of SSEs in ASSBs eliminates the need for flammable liquid electrolytes, thereby mitigating the safety concerns associated with LIBs. Furthermore, the adoption of SSEs enables the use of higher-energy-density electrode

Seongho Jo

Seongho Jo is currently a master's degree student at Sangji University. He received his BS degree in the Department of New Energy and Mining Engineering, at Sangji University. His research area is next-generation electrochemical energy storage devices including lithium–sulfur batteries and solid-state electrolytes.

Seongki Ahn

Seongki Ahn is an assistant professor at the Department of Chemical Engineering, at Hankyong National University. He received his PhD in electrochemistry from Waseda University, Tokyo, Japan in 2017, as a recipient of the Monbukagakusho (MEXT) scholarship for his PhD His main research interest is electrochemistry energy storage devices such as Li secondary batteries, electrochemical-double layer capacitors, and hybrid capacitors.

Jun-Woo Park

Jun-Woo Park is currently an associate professor at the University of Science and Technology. He earned his Master's and PhD degrees under the guidance of Professor Masayoshi Watanabe at Yokohama National University, Japan, as a recipient of the prestigious Monbukagakusho (MEXT) Scholarship. He is an expert in the field of electrochemical materials and next-generation rechargeable batteries. Since 2013, he has been a Principal Researcher at the Battery Research Division of the Korea Electrotechnology Research Institute (KERI). His research focuses on sulfur-based solid-state electrolyte, cost-effective fabrication of all-solid-state batteries, and redox flow batteries.

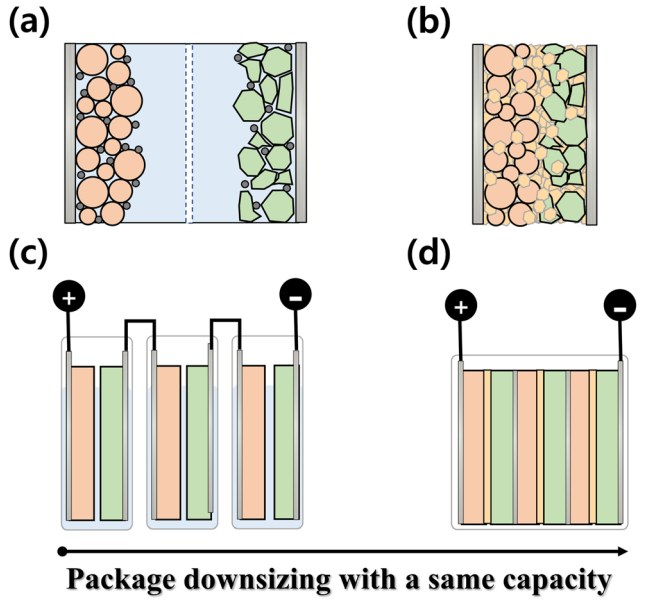

Fig. 1 Schematic illustration of a (a) conventional LIB with liquid electrolyte and (b) ASSB, and batteries with (c) liquid electrolytes and (d) SSEs.

materials, potentially leading to increased energy storage capacity. With ongoing research and development efforts, ASSBs have significant potential to revolutionize the field of electrochemical energy storage and serve as viable replacements for conventional LIBs.

The differences between conventional LIBs and ASSBs are illustrated in Fig. 1(a) and (b). In a conventional LIB system, a cell is prepared using a liquid electrolyte and a separator. The conventional organic liquid electrolytes used in LIBs exhibit desirable physical and electrochemical properties, including high lithium-ion conductivity and reactivity with the cathode and anode during the charge/discharge process. However, it has significant disadvantages such as poor thermal stability and potential leakage issues.[68–70] The poor thermal stability of organic liquid electrolytes can lead to thermal runaway and safety hazards, particularly under extreme conditions or during battery abuse. The flammability of electrolytes increases the risk of fire incidents and compromises the overall safety of EVs.[71–75] Moreover, electrolyte leakage can result in performance degradation, energy density loss, and compromised durability of battery systems (Fig. 1(c)). These shortcomings pose critical challenges, particularly in EV applications.[76]

Unlike conventional LIBs, ASSBs employ SSEs in their cell configuration. This unique design feature offers several advantages, including the ability to reduce cell thickness. As illustrated in Fig. 1(d), this reduction in thickness allows the downsizing of the battery cell, module, and pack, which can increase the volumetric energy density. By decreasing the overall volume of battery components, more energy can be packed into a given volume, resulting in higher volumetric energy density than conventional LIBs. This is a significant advantage for applications where space is limited, such as EVs, as it allows for greater energy storage capacity within a smaller footprint, making them highly attractive for various applications requiring high energy density in a compact form.

This review article primarily focuses on the challenges and research trends surrounding ASSBs, in the context of productivity, cost, eco-friendliness, and important strategies, with the aim of facilitating their commercialization. Additionally, we explore the potential applications of all-solid-state electrolytes in next-generation batteries, including lithium–sulfur, sodium-ion, and magnesium-ion batteries. The key points discussed in this review are the: (a) crucial considerations for the commercialization of ASSBs, (b) strategies for addressing these challenges, and (c) alternative applications for solid electrolytes (SE). This comprehensive review offers valuable insights and guidance regarding important strategies and solutions for the successful commercialization of ASSBs.

2. Strategies for ASSB membrane preparation

2.1. Solid electrolyte synthesis

Various SSEs have been investigated for potential applications. For example, oxide-based electrolytes, such as garnet-type $Li_3La_3Zr_2O_{12}$ (LLZO), offer excellent chemical stability and high ionic conductivity (approximately 1 mS cm^{-1}), making them promising candidates for ASSBs. Halide-based electrolytes, such as Li_3YCl_6 and Li_3YBr_6, exhibit high ionic conductivity and good stability but may face challenges related to their chemical reactivity. Sulfide-based electrolytes, such as Li_6PS_5Cl (LPSCl), demonstrate both high ionic conductivity and good mechanical properties, making them attractive for solid-state battery applications. Polymer-based electrolytes, such as polyethylene oxide (PEO)-based electrolytes, provide flexibility and processability; however, their relatively low ionic conductivities pose challenges for high-performance batteries.[77–87] Intensive research is currently being conducted on materials for SEs that exhibit high ionic conductivities. However, challenges concerning their dry synthesis methods (*e.g.*, high-energy ball milling), high production costs, and large-scale synthesis must be addressed for the commercialization of these materials.

Recent studies have highlighted the current research trends in SEs and the major obstacles hindering their commercialization. Ongoing research is primarily focused on enhancing the ionic conductivity of SEs, which is critical for the efficient movement of ions in these materials. Many studies reference existing methods such as high-energy ball milling, a dry fabrication technique that allows the synthesis of high-purity SEs with high ionic conductivities by minimizing impurities. However, this process consumes substantial energy, leading to high production costs and limiting large-scale production. To facilitate the commercialization of solid-state batteries, researchers have been investigating methods to reduce costs and enable the mass production of SEs for use in a broad range of applications.

2.1.1. Mass production. Wet synthesis methods for SSEs have been developed to overcome the limitations of dry processing methods. These offer advantages such as improved homogeneity, better control over particle size and morphology, and the ability to produce large-scale sulfide-based electrolytes

for commercial-scale production. Many studies have actively investigated wet synthesis approaches, such as additive, sol–gel, hydrothermal, solvent selection, and precipitation methods, to optimize the synthesis of sulfide-based SSEs.[88–95] Ito *et al.* introduced a wet fabrication method to synthesize a $Li_7P_3S_{11}$ SE using 1,2-dimethoxyethane (DME) as the solvent because of its ability to coordinate with lithium ions and suitability for industrial applications.[96] The precursor for $Li_7P_3S_{11}$ was prepared by mixing the Li_2S and P_2S_5 powders in DME. After vacuum drying, the precursor was crystallized into $Li_7P_3S_{11}$ by heat treatment in an argon atmosphere at temperatures between 200 °C and 300 °C. X-ray diffraction (XRD) patterns confirmed the formation of crystalline $Li_7P_3S_{11}$ after heat treatment at 200 °C and 250 °C. The synthesized $Li_7P_3S_{11}$ samples exhibited increased ion conductivity (2.7×10^{-4} S cm^{-1} at 25 °C) after heat treatment. However, residual organic solvents present in the generated SE hinders lithium-ion transport, resulting in low ion conductivity and high activation energy. Xu *et al.* manufactured Li_2S–P_2S_5 glass-ceramics using tetrahydrofuran (THF), acetonitrile (ACN), and a mixture of THF and ACN as solvents. The resulting product heated at 250 °C exhibited ion conductivity of up to 9.7×10^{-4} S cm^{-1} at 25 °C.[97]

The aforementioned studies involved significant time consumption for the reaction between the solvents and precursors, leading to substantial time wastage in the synthesis of SEs. Phuc *et al.* rapidly advanced the reaction between Li_2S and P_2S_5 by mixing LiI and P_2S_5 and conducting the reaction in ethyl propionate solvent.[98] To accelerate the synthesis kinetics of the precursor, P_2S_5 and LiI were mixed to form a solution, and Li_2S was added to synthesize the SE. Based on the XRD analysis results, with the exception of a small unknown peak located at $2\theta \approx 20.2°$, the other peaks primarily exhibited the characteristics of $Li_7P_2S_8I$. Furthermore, this unknown peak was observed only in samples synthesized over short times (30, 45, and 60 min)

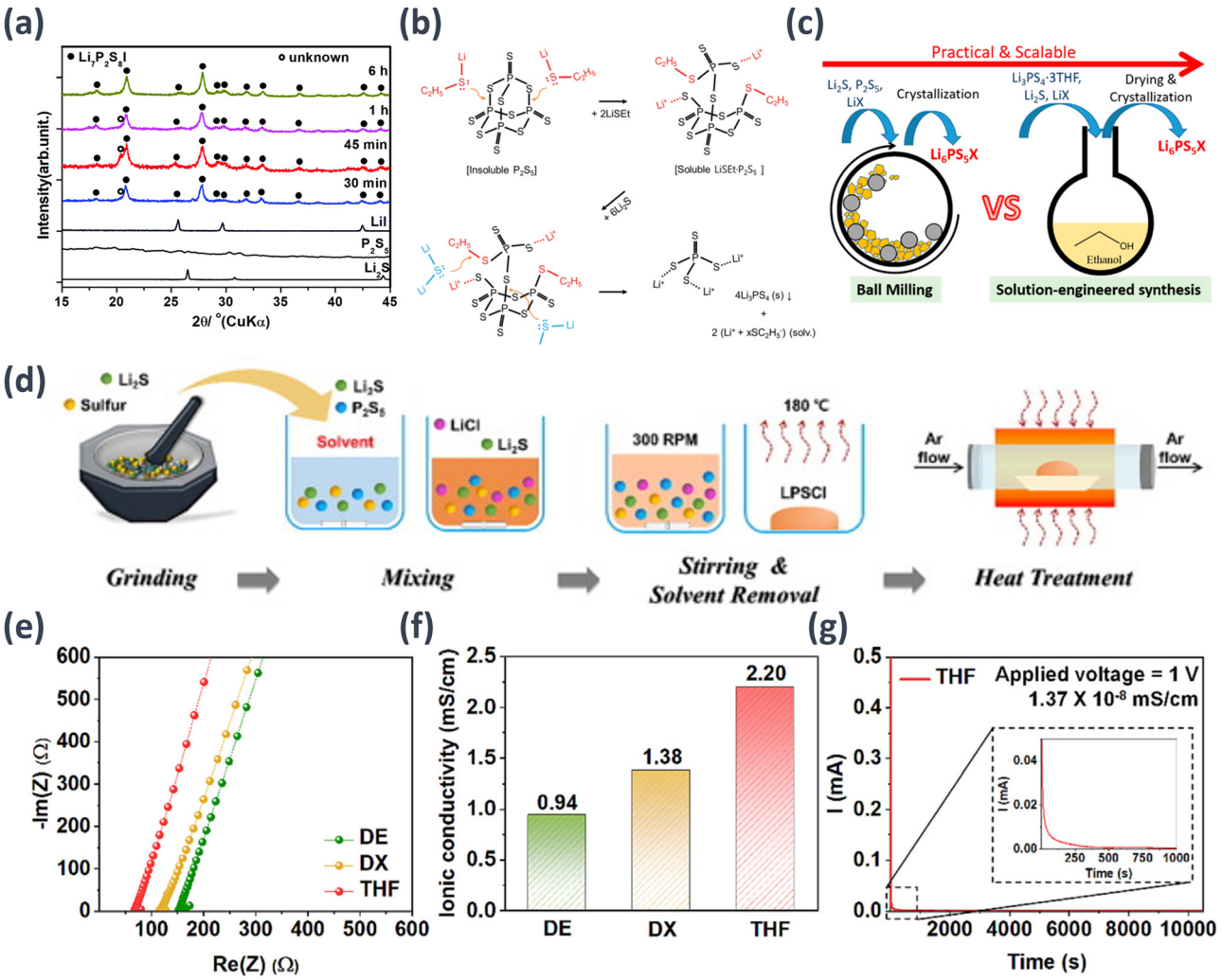

Fig. 2 Schematic examples of SE synthesis methods and results: (a) XRD patterns of the initial components and LPSI (x = 0) prepared at various times after drying at 170 °C for 2 h.[98] (b) Formation processes of Li_3PS_4 SE facilitated by a nucleophilic, $LiSC_2H_5$.[99] (c) Li_6PS_5X (X = Cl, Br) synthesized through ball milling and solution-engineered synthesis techniques.[101] Reprinted (adapted) with permission from ref. 101, Copyright 2018 American Chemical Society. (d) Liquid-phase synthesis process for LPSCl SEs, (e) Nyquist plots and (f) ionic conductivities for various LPSCl SE. (g) Direct current (DC) polarization curve of THF-SE under an applied voltage of 1.0 V.[100]

and disappeared in samples prepared for 6 h, suggesting that it is an intermediate substance. As the reaction time extended, this intermediate appeared to transform into LPSI. This mechanism reduced the reaction time to 30–60 min by enhancing the synthesis kinetics of the precursor (Fig. 2(a)).

In the synthesis of sulfide-based SEs such as LPS and LPSCl, P_2S_5 is commonly used as the source material. However, its insoluble nature and tendency to form a P_4S_{10} case structure limit its potential for SE synthesis. To address this challenge and enable the rapid solution synthesis of thiophosphate electrolytes, a solvent that either dissolves or reacts first to form a soluble complex must be employed, thereby disrupting the cage structure to initiate the reaction. In the pre-reaction step, a strong nucleophilic agent, lithium thioethoxide (LiSEt), was used. LiSEt reacted with P_4S_{10} to form a completely soluble complex. Subsequently, it reacted with Li_2S to synthesize Li_3PS_4. This approach enables the efficient synthesis of thiophosphate electrolytes by circumventing the limitations associated with P_2S_5 and achieving soluble complex formation. The utilization of LiSEt as a nucleophile agent contributes to the successful synthesis of β-Li_3PS_4 SE (1.32×10^{-4} S cm^{-1}), an important SE material for advanced battery systems (Fig. 2(b)).[99]

However, SEs obtained *via* wet synthesis continue to display limited ionic conductivities. Therefore, researchers have aimed to produce SEs with improved ionic conductivity. For example, in making a type of SE called argyrodite Li_6PS_5Cl using wet fabrication methods, the optimal solvent to achieve elevated ionic conductivity must be used. Choi *et al.* found that the choice of solvent significantly affected the purity, crystallinity, and conductivity of the resulting SEs. The Choi group compared different solvents and discovered that THF led to the highest solubility of the precursor materials and the formation of highly conductive crystalline LPSCl SEs. These THF-processed SEs exhibited a maximum ionic conductivity of 2.20 mS cm^{-1} at 25 °C. All-solid-state lithium batteries were fabricated using THF-processed LPSCl SEs, and their electrochemical performance was evaluated. These cells exhibit excellent rate capabilities and cycling stabilities at various current densities, demonstrating the potential of the developed THF-processed SEs for high-performance all-solid-state lithium batteries (Fig. 2(d)–(g)).[100] Moreover, some researchers have also presented the use of solvent mixtures, enabling a broader range of solvent choices other than nonpolar solvents. Zhou *et al.* introduced a solution-engineered method for synthesizing other argyrodite-type SEs, including a new argyrodite solid-solution phase, $Li_{6-y}PS_{5-y}Cl_{1+y}$ (y = 0–0.5), in addition to Li_6PS_5Cl.[101] This method involves dissolving $Li_3PS_4{\cdot}3THF$, Li_2S, and LiX (X = Cl, Br, I) in a mixture of THF and ethanol to synthesize Li_6PS_5X materials. The resulting materials exhibited high ion conductivities with a maximum of 3.96 mS cm^{-1}. These findings present a novel perspective on the mass synthesis of ASSB SEs for commercialization (Fig. 2(c)).

2.1.2. Cost. The development of solid-state batteries, aimed at replacing traditional liquid electrolyte-based batteries, is progressing through numerous exceptional research efforts to achieve ion conductivity levels comparable to those of liquid electrolytes. However, despite these advancements, solid-state batteries still face challenges in terms of commercialization due to cost-related factors. Their production cost remains higher than that of conventional liquid electrolyte batteries, primarily because of the complexity introduced by the development and optimization of new manufacturing processes, high costs associated with specialized materials to meet the requirements of high performance and safety, and factors such as rising raw material prices (Table 1).[93] Consequently, this review focuses on mitigating these challenges to enable commercialization by reducing process complexity or altering synthesis materials, ultimately leading to lower production costs.

Currently, sulfide SEs have been gaining attention because of their high ion conductivity and significant ductility. However, their commercialization faces a hurdle owing to the high cost of a key raw material, lithium sulfide (Li_2S), in their manufacturing process. Tu *et al.* focused on the development of a low-cost and scalable synthesis method for high-purity Li_2S involving the carbothermic reduction of lithium sulfate with different raw material mixing methods to improve the reaction efficiency. Ethanol was then used to purify Li_2S, and the subsequent calcination temperature was optimized to obtain a high-purity product. Their low-cost and scalable synthesis method offers a practical solution for producing high-purity

Table 1 Comparison of the price of final battery cells, manufactured all-solid-state-batteries using the conventional solid electrolytes, and conventional lithium-ion-batteries with liquid electrolyte

Components	Weight in a cell [g]	Unit price [$ per kg]	Cost [$]	Price ratio [%]	ASSB (conventional SEs)	Conventional LIBs
NCM811	31.613	22	0.6955	12.4	695.5	185.69
Carbon black	1.317	35	0.0461	0.82	46.1	4.57
Binder	1.317	65	0.0856	1.53	85.62	8.48
Al foil	2.207	8	0.0177	0.31	17.66	11.04
Gr	0	0	0	0	0	45.75
SBR	0	0	0	0	0	10.3
CMC	0	0	0	0	0	0.69
Ni foil	4.769	10	0.0477	0.85	47.69	29.38
Separator	7.199	271.6	1.9551	34.85	1955.14	74.81
Electrolyte	9.66	277.1	2.6769	47.72	2676.85	64.5
Al pouch	2.24	17	0.0381	0.68	38.08	6.78
Lead tab (+)	0.156	300	0.0469	0.84	46.92	4.5
Lead tab (−)	0.455	200	0.0909	1.62	90.92	9.6
Total weight [g]	60.478		5.6096	100	5700.5	456.1

Li_2S. By considering the complete conversion of Li_2SO_4 to Li_2S as the theoretical yield and the obtained pure lithium sulfide (PLS) as the actual output, the yield of PLS was calculated to be 81.08%, which is significantly higher than the yield achieved with dry-mixing and ball-milling methods (71.18%). The current market price of Li_2SO_4 is \$17 per kilogram, while the cost of sucrose is less than \$1 per kilogram. With an impressive yield of 81.08%, the raw material cost for PLS amounts to approximately \$62 per kilogram. Even when considering labor and electricity costs, the overall production cost remains significantly lower than the market price of commercially available Li_2S (\$10 000–15 000 per kilogram). These findings highlight the substantial economic benefits of the proposed Li_2S preparation strategy, which has the potential to significantly reduce the production costs of sulfide-based solid-state batteries, making them economically viable for large-scale commercialization. The high-purity Li_2S synthesized using this method shows promise for enhancing the performance and reliability of solid-state batteries, contributing to the advancement of sustainable energy storage technologies (Fig. 3(a)).[102]

To overcome the hurdles associated with the commercial use of LPSCl SE, Kim *et al.* introduced a readily processable bulk-type solution-based synthesis method that eliminates the need for high-energy ball milling. By incorporating elemental sulfur during preparation, polysulfides are formed from Li_2S and S, facilitating the reaction of P_2S_5 to yield LPSCl with an outstanding ion conductivity of up to 1.8 mS cm^{-1}. The purity of the bulk-type precursors did not affect the final composition or ionic conductivity of the sulfide electrolytes, which demonstrated electrochemical characteristics comparable to those of ASSB cells, with a high discharge capacity of 185.6 mA h g^{-1}.

At present, the cost ratio of liquid electrolytes to that of the conventional LIBs is approximately 14%. Therefore, the price ratio of SEs must be significantly decreased to at least be comparable to that of LIBs to commercialize ASSBs. Kim *et al.* presents a promising strategy to significantly reduce the production costs of sulfide SEs potentially up to 92% by employing low-cost and less pure precursors for large-scale SE production through a solution-based approach. The proposed method has potential for the mass production of high-capacity and low-cost ASSBs that satisfy the electrochemical performance requirements for highly stable EVs and ESS. Moreover, commercial ASSBs adopting this approach are expected to achieve a competitive cost per unit energy density of approximately 0.46 \$ per W. This will be of great interest to those seeking a cost-effective mass production solution for sulfide-based SEs in commercial ASSB applications by minimizing unnecessary steps (Fig. 3(b) and (c)).[103]

One alternative method for synthesizing LPSCl uses a high-cost sulfide-based electrolyte instead of expensive Li_2S. This method involves a metathesis reaction between inexpensive

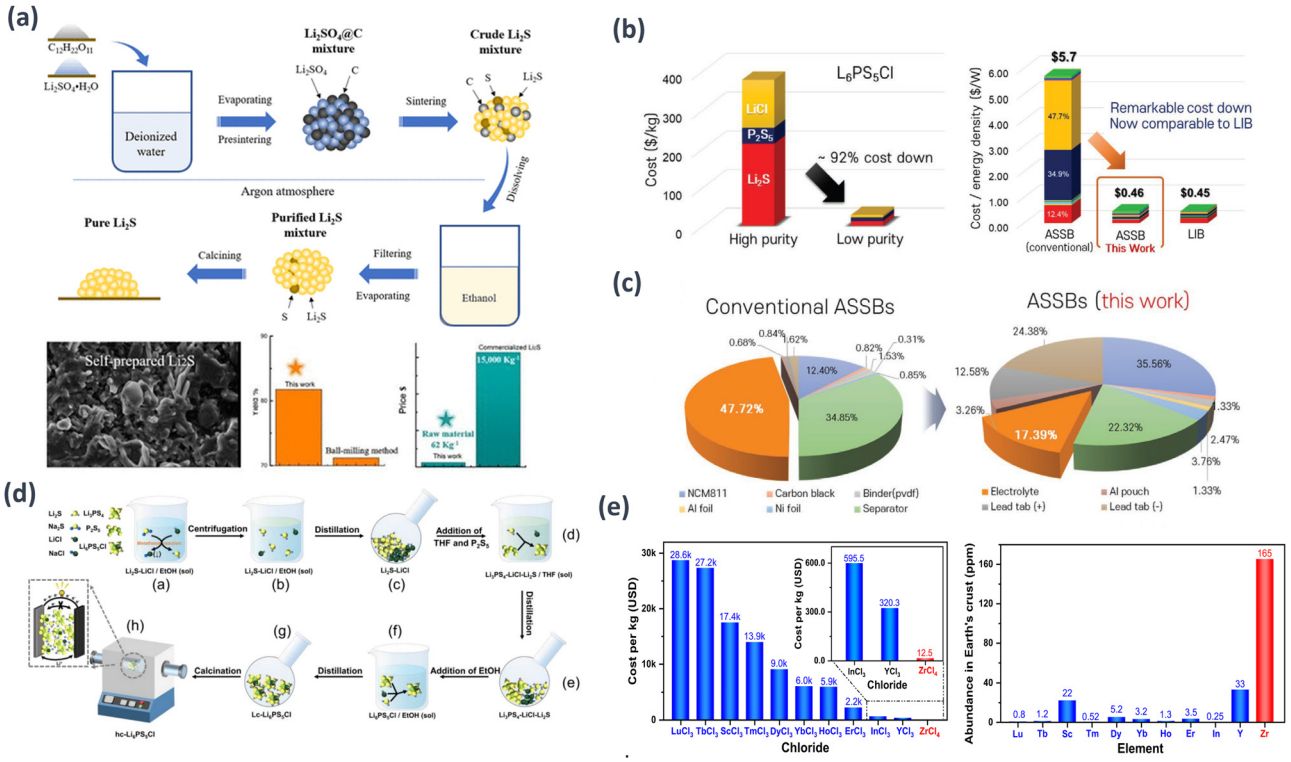

Fig. 3 Schematic examples of SE cost reduction methods and results: (a) Li_2S synthesis approach and minimization of expenses related to raw materials.[102] Reprinted (adapted) with permission from ref. 102, Copyright 2022 American Chemical Society. (b) Comparison of the price of the final battery cells, considering the production of ASSBs employing the traditional SEs and proposed sulfide SEs, and traditional LIBs with liquid electrolytes. (c) Price ratios of the components of conventional and proposed ASSBs when the SE takes the highest price and the lowest price.[103] (d) Process of making Li_6PS_5Cl SE.[104] Reprinted (adapted) with permission from ref. 104, Copyright 2022 American Chemical Society. (e) Raw-material cost of Li_2ZrCl_6 and state-of-the-art chloride SEs.[105]

LiCl and Na_2S to produce Li_2S nanocrystals *in situ*. Li_2S is required in both the intermediate Li_3PS_4 and the final product Li_6PS_5Cl, making it advantageous to produce Li_2S in one step to produce Li_6PS_5Cl. Additionally, the use of LiCl as a reactant for Li_2S production eliminates the need for separate recovery of LiCl from Li_2S. The common ion effect facilitated by LiCl enhanced the precipitation of the NaCl byproduct during Li_2S synthesis. The excess Li_2S used in the Li_3PS_4 step was expected to promote faster reaction kinetics. The synthesis strategy involves three stages: (1) adding Na_2S and LiCl in a molar ratio of 5/2 : 6 to ethanol to generate Li_2S, removing the precipitated NaCl, and collecting the remaining Li_2S and LiCl as powder after ethanol distillation; (2) adding P_2S_5 and THF to the Li_2S powder to produce white precipitate Li_3PS_4, and collecting the solid mixture of Li_3PS_4, LiCl, and Li_2S after THF distillation; and (3) dissolving the solid mixture in ethanol recovered from stage 1 to obtain a Li_6PS_5Cl solution, followed by ethanol distillation to obtain lc-Li_6PS_5Cl powder, which is then calcined under argon to obtain hc-Li_6PS_5Cl. This method reduces the material cost by approximately 50 times compared with methods using Li_2S and offers the potential for the low-cost and large-scale production of practical Li_6PS_5Cl electrolytes. The resulting electrolyte demonstrates excellent performance in terms of ionic conductivity (approximately 2 mS cm^{-1}) and cycling stability (over 99.8% capacity retention after 400 cycles at 1C) (Fig. 3(d)).[104]

Halide-based SSEs have gained attention because of the combination of mechanical deformability from sulfides and excellent electrochemical stability from oxides. Wang *et al.* identified new orthorhombic phases by substituting scarce and costly elements, such as Y, Er, Sc, and In, with Zr in halide-based systems. Wang *et al.* focused on the synthesis of novel halide superionic conductors, specifically hexagonal close-packed (hcp) Li_2ZrCl_6 and Fe^{3+}-doped Li_2ZrCl_6, using a cost-effective mechanochemical method with readily available elements. This represents a significant advancement in the field of practical all-solid-state technologies and provides valuable insight into the design of future halide superionic conductors. Wang *et al.* introduces Li_2ZrCl_6 as a cost-effective high-performance chloride SE that can maintain electrochemical performance while using substantially cheaper raw material sets ($1.38 per m^2) than other chloride SEs, making a highly competitive option for practical applications in solid-state batteries. Furthermore, the study underscores the significance of the properties and potential for industrial utilization of Li_2ZrCl_6 (0.81 mS cm^{-1} at room temperature). Through this approach, high-cost sulfide- and chloride-based SEs can be made more affordable, offering a new alternative for the commercialization of ASSBs (Fig. 3(e)).[105]

2.1.3. Eco-friendliness. With a growing global focus on environmental issues, numerous countries are striving for carbon neutrality. This trend highlights the increasing importance of environmentally friendly policies and actions. As research on solid-state batteries has flourished, concerns have arisen about the materials used in synthesizing SEs, including material choices, processing methods, and the potential for environmental contamination during disposal. Therefore, the materials for synthesis must be carefully selected. Prioritizing the use of eco-friendly materials is key to developing sustainable ESS. Making environmentally conscious choices in material selection can contribute toward creating a cleaner and more sustainable future for energy sources. Recent research holds the potential not only for preserving the environment, but also for realizing social and economic benefits.

Although ASSBs offer great potential for high-energy-density energy storage, the development of scalable and environmentally friendly synthesis methods for sulfide electrolytes remains challenging. Researchers have systematically investigated the effects of various green solvents on sulfide electrolyte synthesis by considering factors such as solubility, stability, and reaction kinetics. Jo *et al.* summarized the research on engineering green and sustainable solvents for the scalable wet synthesis of sulfide electrolytes in high-energy-density ASSBs[106] and proposed an innovative approach that focuses on the selection and optimization of green and sustainable solvents for wet syntheses. The use of environmentally friendly solvents not only ensures the sustainability of the battery manufacturing process, but also promotes the synthesis of high-quality sulfide electrolytes with desirable electrochemical properties. The results demonstrate that the choice of solvent significantly influences the morphology, composition, and electrochemical performance of the sulfide electrolytes. By carefully selecting and optimizing green solvents, researchers have successfully fabricated sulfide electrolytes with improved ionic conductivities, enhanced interfacial stabilities, and excellent cycling performances. These findings contribute to the development of sustainable and scalable wet synthesis methods for sulfide electrolytes in high-energy-density ASSBs, opening new avenues for the large-scale production of environmentally friendly ESSs (Fig. 4(a)).

Sustainability refers to the production of batteries using environment-friendly materials *via* sustainable processes. Environmentally friendly materials are abundant, available from renewable resources, and are less toxic or non-toxic. Sustainable processes focus on improving the carbon footprint of production. Lithium iron phosphate ($LiFePO_4$, LFP) is a highly sustainable active cathode material. Ye *et al.* used the interaction of PEO with water *via* hydrophilic interactions involving hydrogen bonding to create water-soluble PEO. By exploiting this property, an LFP–PEO composite cathode was fabricated to induce improved interfacial formation. The influence of various solvents on the PEO was compared to evaluate the water-based processing of the LFP–PEO composite cathode. The battery produced using the LFP–PEO composite cathode achieved a specific capacity of 136 mA h g^{-1} at a current density of 50 μA cm^{-2} in the first cycle (Fig. 4(b)).[107]

Recycling spent batteries, including ASSBs, plays a crucial role in creating eco-friendly environments. Developing innovative recycling processes for lithium recovery is vital for the sustainable management of natural lithium resources and eco-conscious production methods. EV manufacturers are actively exploring opportunities to reuse spent batteries in applications

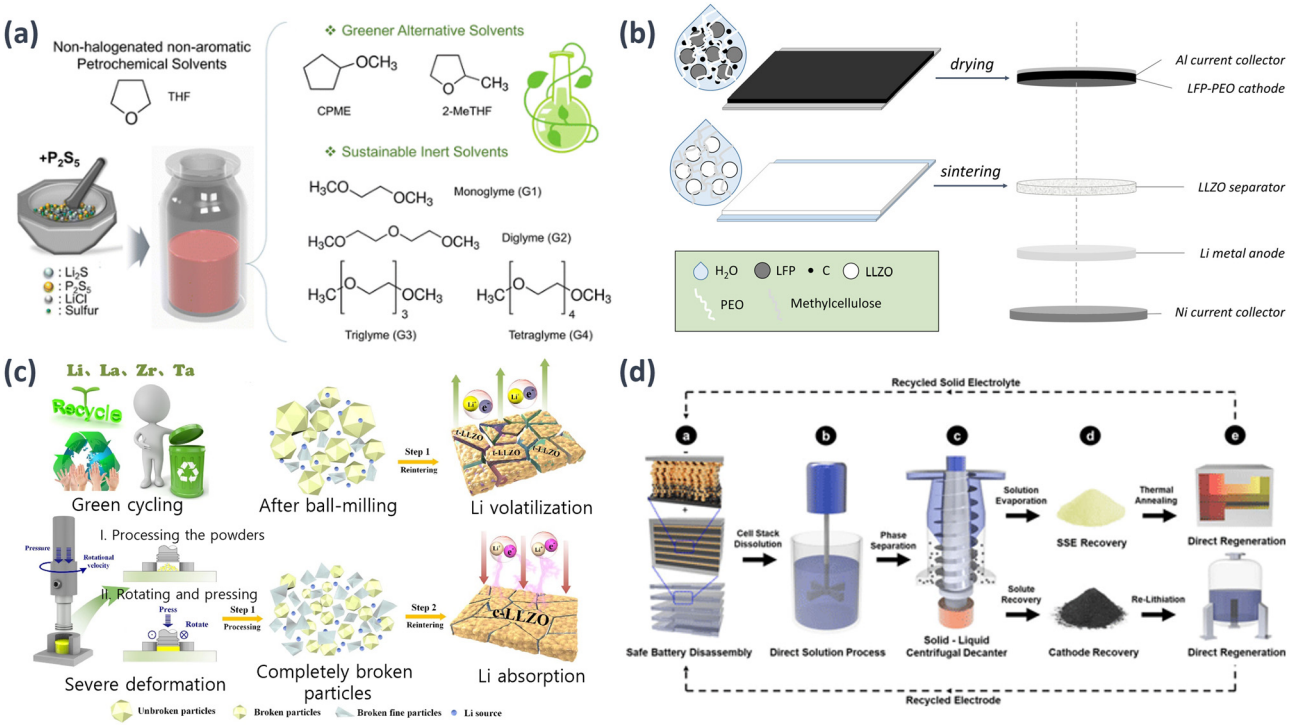

Fig. 4 Schematic examples of sustainability research concerning SEs: (a) liquid-phase synthesis procedure of LPSCl SEs employing different solvent systems, *i.e.*, traditional THF, greener alternative solvents (CPME and 2-MeTHF), and sustainable inert solvents (G1–G4).[106] (b) Water-based manufacturing for the LFP-PEO composite cathode with LLZO separator utilized in SSLBs.[107] Reprinted (adapted) with permission from ref. 107, Copyright 2022 American Chemical Society. (c) Recycling routes.[109] (d) Proposed ASSB recycling procedure at an industry, based on the principles of direct recycling.[110]

such as ESS to maximize their value and reduce industrial waste. The recycling dimensions of ASSBs are currently underexplored but are of utmost importance given the expected increase in the disposal of LIBs, particularly in the automotive sector. The current state of LIB recycling is insufficient, and the introduction of lithium–metal anodes and SE chemistry in ASSBs introduces additional complexities. Thus, recycling and efficient waste management should be prioritized to advance the commercialization of ASSBs.[108] Qin *et al.* explored the recycling potential of SSEs, focusing on solvent sludge and achieved a densification interface with a high lithium-ion conductivity of 3.55×10^{-4} S cm^{-1} at room temperature. The critical current density of the deformation-driven re-sintering (DDR)-SSE reached 1.24 mA cm^{-2}, demonstrating a stable lithium stripping and plating process. The recycled DDR-SSE exhibited superior cycling performance, with a discharge capacity of 126.7 mA h g^{-1} and a capacity retention of 89.7% after 400 cycles (0.5C). SSLBs assembled using recycled DDR-SSE exhibited a desirable performance. The application of the DDR technology for recycling spent SSEs has proven to be an effective way of enhancing the environmental sustainability and economic viability of the battery industry (Fig. 4(c)).[109] Furthermore, Tan *et al.* proposed a scalable recycling model for ASSBs to recover and regenerate SEs and cathode materials from spent batteries and used the EverBatt model to assess the energy consumption and environmental impact of their recycling strategies and compared them with traditional pyrometallurgical and hydrometallurgical methods.[110] The regenerated Li_6PS_5Cl exhibited structural properties and ionic conductivity similar to those of pristine Li_6PS_5Cl and $LiCoO_2$, highlighting the effectiveness of the recycling models (Fig. 4(d)).

2.2. Fabrication techniques

In the commercialization of solid-state batteries, the fabrication technology of the SE membrane layers is a crucial factor. First, within solid-state battery systems, these layers must act as separators to prevent direct contact between the cathode and anode, while also inhibiting the formation of lithium dendrites and addressing the associated stability issues. The prevention of short circuits caused by lithium dendrites is essential because of the potential risks of battery overheating and fire. Through the SE layer, ion transport within the battery is improved, resulting in reduced internal resistance, which, in turn, affects battery performance, including charge–discharge efficiency and capacity retention. Table 2 lists the details of the SSE and cell performances, such as ionic conductivity, thickness, capacity, and cycling performance. In this section, we introduce studies that present fabrication methods for membranes that are crucial for the commercialization of high-safety and high-energy-density solid-state batteries.[111,112]

2.2.1. Thin-film deposition methods. A significant avenue for enhancing the energy density of solid-state batteries is minimizing the weight of the SE layer. Therefore, the thin-film deposition of SE layers is a highly important technology for the commercialization of high-energy-density solid-state batteries. Tan *et al.* fabricated thin electrolyte films (~50 μm) by

Table 2 Comparison of SSE performance of previously reported ASSLBs[abc]

Ref.	SE	Ionic conductivity (mS cm^{-1})	Thickness (μm)	Capacity (mA h g^{-1})	C-Rate	Cyc. (th)	T (°C)
SSE with thin-film deposition methods							
Tan *et al.*[113]	$Li_7P_3S_{11}$	~0.7	~50	ND	ND	ND	ND
Kang *et al.*[114]	Li_6PS_5Cl	1.54	ND	ND	ND	ND	ND
Kim *et al.*[115]	$Li_6PS_5Cl_{0.5}Br_{0.5}$	2	40–70	146	0.1C	100	30
Wei *et al.*[116]	$Li_{6.4}La_3Zr_{1.4}Ta_{0.6}O_{12}$	0.653	~15	150.2	0.5C	269	25
Kang *et al.*[117]	Li_6PS_5Cl	0.55	66	119.1	0.1C	120	60
Zhang *et al.*[118]	$Li_{5.4}PS_{4.4}Cl_{1.6}$	8.4	30	135.3	0.05C	150	60
Reinacher *et al.*[119]	$Li_6BaLa_2Ta_2O_{12}$	1.7×10^{-3}	2	ND	ND	ND	ND
SSE with chemical vapor depostion							
Loho *et al.*[121]	$Li_7La_3Zr_2O_{12}$	4.2×10^{-3}	~1	ND	ND	ND	ND
Li *et al.*[122]	Li_6PS_5Cl	5.1	~60	107	1C	800	ND
Yang *et al.*[123]	F-NBR-*g*-VEC	0.4	ND	130	0.5C	300	30
SSE with atomic layer deposition							
Li *et al.*[125]	$Li_{1.3}Al_{0.3}Ti_{1.7}(PO_4)_3$	0.1	ND	156	0.2C	50	25
Wang *et al.*[126]	Lithium silicate	5.72×10^{-6}	0.049	ND	ND	ND	ND
Jin Su *et al.*[127]	MgPON	1.2×10^{-3}	ND	ND	ND	ND	ND

[a] Some data are inconsistent with those in the literature, which is mainly caused by the calculation according to our formula standard for the convenience of comparison and uniformity. [b] "ND" means no valid data can be obtained from the literature. [c] We selected the data with cycling performance (>10 cycles) for the comparison and excluded the data with only rate performance and without cycling performance.

blending an $Li_7P_3S_{11}$ SSE with low dielectric constant and polar p-xylene with a corresponding polymer without electronegative functional groups such as Styrene Ethylene/Butylene Styrene (SEBS). The composite electrolyte membrane demonstrated electrochemical stability during the lithium plating and stripping processes (2000 h, 1.1 mA h cm^{-2} per cycle), enabling the use of metallic lithium anodes in ASSBs. Additionally, the incorporation of hydrophobic SEBS enhanced the air moisture stability of $Li_7P_3S_{11}$. The SSE–polymer–solvent selection principles used can be extended to other SSE–polymer–solvent compositions and further optimized to achieve superior performance. Furthermore, the insights gained from this research offer a new material selection philosophy that can lead to the development of scalable methodologies for producing high-performance and cost-effective ASSBs (Fig. 5(a)).[113]

Kang *et al.* employed a scalable and cost-effective liquid-phase process to fabricate a 2D structured argyrodite LPSCl SE using ACN as the solvent and reduced graphene oxide (rGO) as the template to overcome the restricted surface applicability of active materials and a constrained conductive network within composite electrodes due to the spatial confinement of SE particles.[114] The favorable ion percolation resulting from the high aspect ratio of the SE particles led to a threefold enhancement in the effective ion conductivity within the composite electrode (1.54 mS cm^{-1}) (Fig. 5(b)). Kim *et al.* successfully developed thin, flexible, and highly conductive single-ion conducting SE membranes that exhibited exceptional thermal stability for application in ASSBs by employing an innovative technique of infiltrating solution-processable Li_6PS_5[Cl,Br] into electrospun porous PI nanowire scaffolds.[115] The $LiNi_{0.6}Co_{0.2}Mn_{0.2}O_2$/graphite ASSBs with 40 μm thick $Li_6PS_5Cl_{0.5}Br_{0.5}$-infiltrated PI membranes demonstrated a promising performance at 30 °C, boasting a specific capacity of 146 mA h g^{-1}, and showcased remarkable thermal stability with minimal degradation even at elevated temperatures of up to 180 °C. Although the energy and power densities demonstrated may not yet compete with cutting-edge LIB technologies, these proof-of-concept results provide valuable insights into the developmental principles of SEs, particularly regarding the practical scalability of ASSB manufacturing (Fig. 5(c)).

Solid-state lithium–metal batteries (LMB) hold great promise for next-generation energy storage owing to their high energy density and improved safety. However, low ionic conductivity and poor interfacial stability hinder their practical application. Wei *et al.* proposed an ultrathin solid composite electrolyte to address these challenges. It had $Li_{6.4}La_3Zr_{1.4}Ta_{0.6}O_{12}$ as the SSE with high ionic conductivity, polyvinylidene fluoride-hexafluoropropylene (PVDF-HFP) as a binder, and lithium bis(trifluoromethane)sulfonimide (LiTFSI) and succinonitrile to provide enhanced ionic transport properties.[116] The composite electrolyte was fabricated as an ultrathin film that exhibited excellent electrochemical performance, including high ionic conductivity, low interfacial resistance, and good cycling stability, thereby enabling efficient lithium-ion conduction and improved interfacial stability. When incorporated into solid-state LMBs, the composite electrolyte enables high-performance and long-lasting battery operation (Fig. 5(d)). Kang *et al.* created an ultrathin SE membrane that can be reduced to a thickness of 31 μm without significant thermal shrinkage at 140 °C.[117] The membrane exhibited excellent mechanical properties, including a tensile strength of 19.6 MPa. Argyrodite sulfide SE, LPSCl with an ionic conductivity of 1.7 mS cm^{-1} in pellet form, nonpolar solvent, toluene, and a nitrile butadiene rubber (NBR) binder were used to produce SE slurries that were applied to a nylon net template using the conventional doctor blade coating technique. Notably, the integrated SE membrane within an anode-supported battery showcased remarkable ionic conductivity (0.55 mS cm^{-1}) and areal conductance (84 mS cm^{-2}), significantly improving energy densities at the cell level. It measured 127.9 W h kg_{cell}^{-1} gravimetrically and 140.7 W h L_{cell}^{-1} volumetrically, representing impressive 7.6-fold and 5.7-fold increases, respectively, compared with conventional SE pellet cells (Fig. 5(e)).

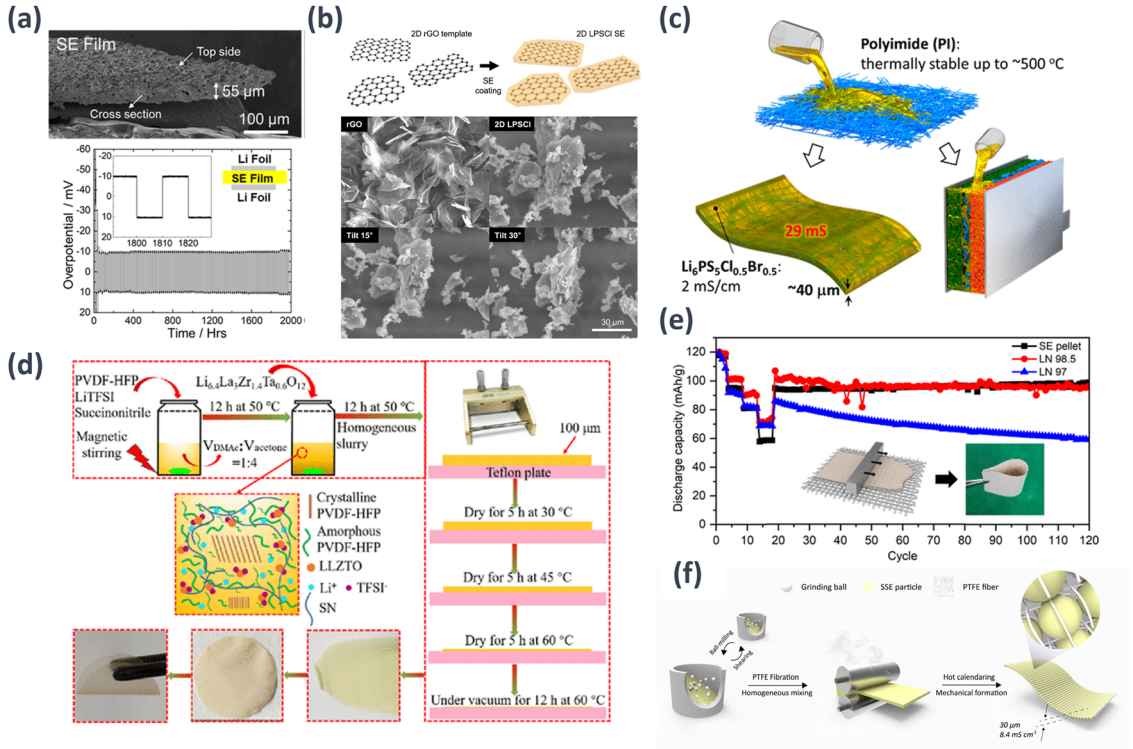

Fig. 5 Schematic examples of thin-film deposition methods: (a) cross-section SEM image of composite electrolyte film fabricated with 95 wt% $Li_7P_3S_{11}$ and 5 wt% SEBS. This film underwent lithium plating and stripping over 100 cycles at 20 h per cycle.[113] Reprinted (adapted) with permission from ref. 103, Copyright 2019 American Chemical Society. (b) 2D LPSCl SE and SEM images of rGO template and 2D LPSCl SE at different tilted angles.[114] (c) Fabrication of sulfide SE membranes for ASLBs through the infiltration of electrospun porous PI nanowires with solution-processable $Li_6PS_5[Cl,Br]$.[115] Reprinted (adapted) with permission from ref. 105, Copyright 2020 American Chemical Society. (d) Preparation of solid composite electrolyte membranes.[116] Reprinted (adapted) with permission from ref. 116, Copyright 2020 American Chemical Society. (e) Cycle performance of ASSB cells assembled with SE pellet or SE membrane and fabrication of SE membrane with nylon net membrane.[117] Reprinted (adapted) with permission from ref. 117, Copyright 2023 American Chemical Society. (f) The fabrication of ultrathin SE membrane.[118] Reprinted (adapted) with permission from ref. 118, Copyright 2021 American Chemical Society.

Zhang *et al.* successfully constructed a 30 μm sulfide SE membrane that exhibited an exceptionally high room temperature conductivity (8.4 mS cm^{-1}) using a sulfide SE powder composed of $Li_{5.4}PS_{4.4}Cl_{1.6}$ (99.8 wt%) and polytetrafluoroethylene (PTFE) powder (0.2 wt%).[118] Through cell testing involving an NCM cathode and the incorporation of an Al_2O_3 interlayer between the SE membrane and lithium, they observed a discharge specific capacity of 135.3 mA h g^{-1} (equivalent to 1.4 mA h cm^{-2}), with an impressive capacity retention rate of 80.2% over 150 cycles. This performance was achieved while maintaining an average coulombic efficiency exceeding 99.5% (Fig. 5(f)). Reinacher *et al.* reported the growth of lithium-ion conductive $Li_6BaLa_2Ta_2O_{12}$ garnet-type thin films using pulsed laser deposition.[119] The $Li_6BaLa_2Ta_2O_{12}$ compound was synthesized as a target material *via* high-temperature solid-state reactions. To compensate for the lithium loss during film growth, bulk target materials composed of $Li_6BaLa_2Ta_2O_{12}$ and a 5 mol% excess of Li_2O were employed. Thin films were grown on MgO (100) substrates by eliminating bulk target materials. The bulk material exhibited electrical conductivity of up to $\sigma = 5.0 \times 10^{-5}$ S cm^{-1} at 25 °C. In contrast, the $Li_6BaLa_2Ta_2O_{12}$ garnet-type films displayed a lower conductivity of $\sigma = 2 \times 10^{-6}$ S cm^{-1} at 25 °C, which is comparable to the ionic conductivity of LiPON (approximately $\sigma = 2 \times 10^{-6}$ S cm^{-1} at the same temperature). The activation energies for the bulk and thin film samples were 0.44 and 0.42 eV, respectively.

2.2.2. Chemical vapor deposition (CVD). CVD is a crucial manufacturing process used in industries, in which thin films are created on substrates by chemically depositing material from a gas phase, known for its ability to provide uniform and adherent coatings on various surfaces. This process involves supplying chemical gases into a reaction chamber, where they react and form solid materials that are deposited as thin films. CVD is regulated by factors such as the vacuum pressure, temperature, and gas concentration, making it a vital technique for advanced material manufacturing (Fig. 6(a)).[120] Loho *et al.* reported the characteristics of garnet-type lithium-ion conducting LLZO SE thin films grown by CO_2-laser assisted CVD.[121] Single-crystal cubic-phase LLZO films grown on Pt exhibited a dense and homogeneous microstructure without cracks. A total lithium-ion conductivity of 4.2 × 10^{-6} S cm^{-1} at room temperature was achieved with an activation energy of 0.50 eV. This represents the highest reported total lithium-ion conductivity value for cubic-phase LLZO thin films to date, approximately ten times higher than that reported for cubic-phase LLZO films manufactured using sputtering and pulsed laser deposition methods (Fig. 6(b)).

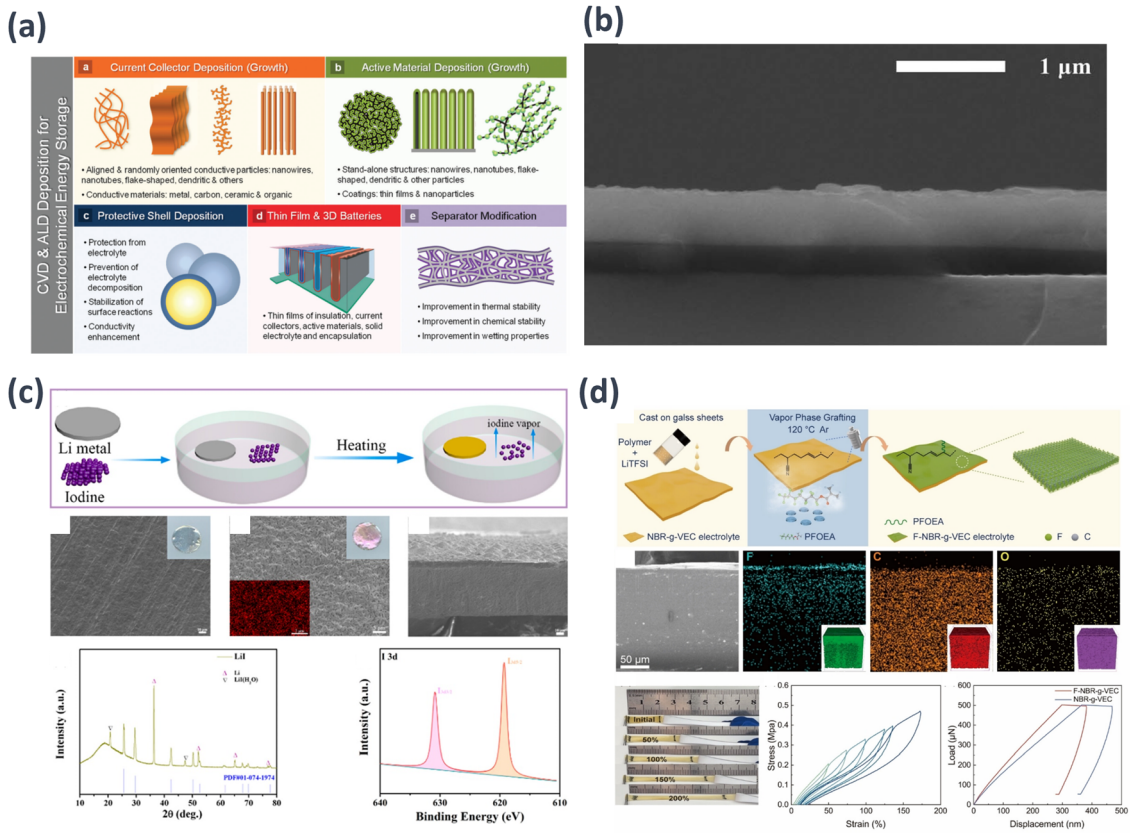

Fig. 6 Schematic examples of the CVD process in: (a) key techniques for energy storage applications.[120] (b) Secondary electron micrographs of LLZO thin films deposited at 973 K and 40% O_2 on Si.[121] (c) Formation of a LiI protective layer on the surface of Li metal and electrochemical analysis of SEM, Cross-sectional SEM, XRD, and XPS.[122] Reprinted (adapted) with permission from ref. 122, Copyright 2022 American Chemical Society. (d) Comprehensive characterization of the F-NBR-*g*-VEC electrolyte and NBR-*g*-VEC membranes.[123]

Li *et al.* utilized CVD to synthesize lithium-ion conductive LiI to enhance the interfacial stability between a sulfide-based SE (*e.g.*, LPSCl) and lithium metal for lithium dendrite growth suppression.[122] The resultant LiI layer exhibited satisfactory ion conductivity and an elevated interfacial energy, as corroborated by density functional theory calculations. In LiI@Li/LPSCl/NCM cells, notably higher discharge capacities of 200 and 107 mA h g^{-1} were achieved at current densities of 0.1 and 1.0C, respectively, surpassing those of Li/LPSCl/NCM cells. Moreover, even after 100 cycles, a discharge capacity of 161 mA h g^{-1} with 84.8% capacity retention was maintained. This can be attributed to the effective hindrance of the reactions between the electrolyte and lithium metal by the protective LiI layer. The pronounced interfacial energy of LiI, which functions as a lithium-ion conductor, not only prevents the growth of lithium protrusions but also facilitates lithium-ion transport (Fig. 6(c)).

Yang *et al.* developed an elastic rubber-derived electrolyte through the electrophilic addition of NBR and a vinyl ethylene carbonate (VEC) monomer in combination with LiTFSI. Subsequently, a fluorine-rich monomer, perfluorooctyl acrylate, was introduced onto the NBR-*g*-VEC electrolyte surface *via* vapor-phase fluorination, resulting in the creation of a lithiophilic elastic electrolyte, termed the F-NBR-*g*-VEC electrolyte. The LiF film formed through CVD established a chemical connection between the electrolyte and lithium anode in LMBs, ensuring dynamic contact maintenance during operation. This facilitates rapid and stable lithium ion movement across the interface, encouraging uniform lithium deposition and suppressing side reactions between the electrolyte components and lithium metal. The novel LMB incorporating this electrolyte demonstrated an exceedingly long cycling lifespan of 2500 h along with a high critical current density of 1.1 mA cm^{-2}. In symmetric lithium cells, outstanding stability was maintained for over 300 cycles throughout the entire cell system (Fig. 6(d)).[123]

2.2.3. Atomic layer deposition (ALD). ALD is a technique capable of the vapor-phase deposition of various thin-film materials. Unlike their counterparts in CVD, ALD processes involve the alternating exposure of chemical precursors for reactions to occur, resulting in the formation of desired materials. This is typically achieved at significantly lower temperatures. A typical ALD process is illustrated in Fig. 7(a). This enables the deposition of materials at the atomic layer level, allowing precise control of the thickness and structure. ALD is characterized by an even and uniform deposition of atoms in each reaction, ensuring a consistent and controlled film thickness. A key advantage of ALD is that it operates without the need for catalysts, and reactions occur at the atomic layer level.

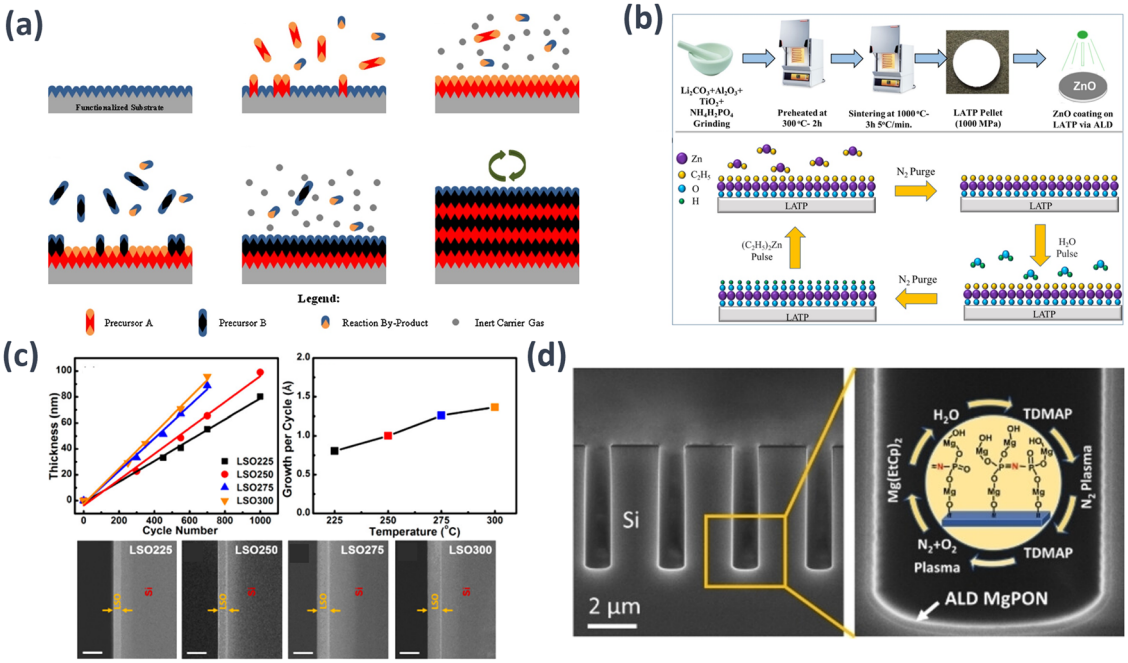

Fig. 7 Schematic examples of the ALD technique in: (a) a naturally functionalized substrate surface or treated for functionalization, in which precursor A reacts with the surface in pulses; excess precursor and by-products are purged with inert carrier gas; precursor B reacts with the surface in pulses; excess precursor and by-products are purged with inert carrier gas, and this cycle is repeated until reaching the desired material thickness.[124] (b) Preparation of LATP modified with ZnO and deposition of ZnO onto the LATP.[125] (c) LSO thin films plotted against ALD cycle number; growth per cycle of LSO at different deposition temperatures; SEM pictures of the cross section of LSO thin films on silicon at 225 °C (LSO225), 250 °C (LSO250), 275 °C (LSO275), and 300 °C (LSO300) after 500 ALD cycles. The scale bar is 100 nm.[126] Reprinted (adapted) with permission from ref. 126, Copyright 2017 American Chemical Society. (d) Reaction steps in one cycle of ALD MgPON SSEs from TDMAP, N_2 plasma, N_2 + O_2 plasma, $Mg(EtCp)_2$, and H_2O precursors. The central inset illustrates the proposed chemical structure of one ALD cycle deposition on the top surface of MgPON SSE films.[127]

Moreover, it can be applied to various materials including insulators, semiconductors, metals, and organic substances. It is a low-temperature process that is suitable for heat-sensitive materials and has significant applications in the semiconductor and nanotechnology fields, particularly for creating layered thin films and manufacturing nanostructured materials. ALD is particularly essential in situations requiring the precise control of film thickness and structure, making it a technology for producing highly reliable thin films (Fig. 7(a)).[124]

Recently, notable instances of implementing ALD processes in the field of membranes have been reported. For instance, Li *et al.* coated a NASICON-type SE $Li_{1.3}Al_{0.3}Ti_{1.7}(PO_4)_3$ (LATP) with ZnO to enhance its interfacial reactions; its bulk structure remained unchanged.[125] The optimized cycle count for the ZnO-ALD coating on the LATP was 50 cycles, resulting in an amorphous characteristic of ZnO and a thin coating of 2.5 nm. The coated ZnO@LATP samples thus exhibited improved interfacial resistance and reduced lithium dendrite formation, leading to a gravimetric capacity of 156 mA h g^{-1} at 0.2C (Fig. 7(b)). In addition, Wang *et al.* employed ALD to fabricate thin films of lithium silicate, a promising SSE for ASSBs.[126] The deposition process for lithium silicate involves sequential ALD cycles of Li_2O and SiO_2, with lithium tert-butoxide, tetraethylorthosilane, and H_2O as precursor materials. This approach yielded a uniform and self-limiting growth pattern within the temperature range of 225 to 300 °C. Employing a one-to-one subcycle of Li_2O and SiO_2 led to thin films approximating Li_4SiO_4 in composition, whereas an additional subcycle of Li_2O resulted in a higher lithium content. The fabricated lithium silicate thin film, synthesized at 250 °C, demonstrated an ionic conductivity of 1.45×10^{-6} S cm^{-1} at 373 K. This demonstrated its potential as an efficient ionic conductor at elevated temperatures (Fig. 7(c)).

Jin Su *et al.* employed a plasma-enhanced ALD system to fabricate magnesium phosphorus oxynitride (MgPON) thin films for magnesium ion-conducting SSEs. The double nitrogen plasma process can be regarded as a nitrogen doping strategy that utilizes radio frequency nitrogen plasma as a nitrogen precursor and proceeds twice in a pulsed manner.[127] Using this approach, nitrogen-incorporated MgPON SSE thin films were synthesized at a low deposition temperature (125 °C). The ALD MgPON SSEs were successfully developed using this method, demonstrating an ionic conductivity of 0.36 and 1.2 μS cm^{-1} at 450 and 500 °C, respectively. This underscores the potential of the ALD-prepared MgPON SSEs as efficient ionic conductors at elevated temperatures (Fig. 7(d)).

3. Strategies for ASSB electrode fabrication

The strategy for electrode fabrication is a crucial factor in the commercialization of solid-state batteries. Electrodes used in

Table 3 Comparison of the cell performance of previously reported ASSLBs[abc]

Ref.	Cathode			Anode	SE (μm)	Capacity (mA h g^{-1})	C-Rate	Cyc. (th)	T (°C)
	CAM (wt%)	Carbon (wt%)	Other (wt%)						
Electrode with dry fabrication									
Hippauf *et al.*[129] Zhang *et al.*[130] -LIB	NCM90 (84.9)	VG-CNF (1.9)	SSE(12.9) PTFE (0.3)	Graphite	Li_6PS_5Cl (150)	184	0.7 mA cm^{-2}	100	25
Yan *et al.*[131] Ludwig *et al.*[132]-LIB	NCM811 (79.4)	VGCF (3)	SSE(16.9) PTFE (0.7)	Si PTFE LiSH	Li_6PS_5Cl (650)	123.6	1C	5000	55
Electrode with wet-slurry fabrication									
Oh *et al.*[133]	NCM71515 (75)	Super C65 (1)	SSE(24.5) NBR(0.75) poly(1, 4-butylene adipate)(0.75) LiTFSI (3)	Graphite SE NBR poly(1, 4-butylene adipate) LiTFSI	$Li_6PS_5Cl_{0.5}Br_{0.5}$ NBR poly(1, 4-butylene adipate) LiTFSI (~600)	160	0.1C	145	30
Yamamoto *et al.*[134]	NCM333 (80)	AB (2)	pulverized fine Li_3PS_4 glass(20) poly(propylene carbonate) (3)	Li–In	Li_3PS_4 glass (10)	149	0.17C	175	30
Kim *et al.*[135]	NCM71515 (70)	Super C65 (1.5)	$Li_6PS_5Cl_{0.5}Br_{0.5}$(21) PvdF-HFP (2.5)	Graphite $Li_6PS_5Cl_{0.5}Br_{0.5}$ PvdF-HFP Super C65	$Li_6PS_5Cl_{0.5}Br_{0.5}$ (150)	160	0.5C	200	30
Kwon *et al.*[136]	NCM71515 (70)	Super C65 (1)	$Li_6PS_5Cl_{0.5}Br_{0.5}$(27.5) PvdF-HFP (1.5)	LTO $Li_6PS_5Cl_{0.5}Br_{0.5}$ NBR	$Li_6PS_5Cl_{0.5}Br_{0.5}$ (600)	153	0.2C	150	30
Electrode with infiltration fabrication									
Kim *et al.*[139]	LCO (97)	Super P (2)	SSE PVDF (1)	Graphite PVDF SSE	Li_6PS_5Cl-nonwoven (70)	100	6C	100	100
Kim *et al.*[142]	NCM622 (96)	Super P (2)	SSE PVDF (2)	Li–In	Li_6PS_5Cl (800)	140	0.1C	30	30
Duchêne *et al.*[144]	$NaCrO_2$ (90)	Super P (5)	SSE PVDF (5)	Sn metal PVDF Super P	$Na_4(B_{12}H_{12})(B_{10}H_{10})$ (500)	634	0.5C	50	30
Song *et al.*[141]	LCO (97)	Super C65 (2)	PVDF(1)	Li–In	$Li_6PS_5Cl_{0.5}Br_{0.5}$ (600)	135	0.2C	100	30

[a] Some data are inconsistent with those in the literature, which is mainly caused by the calculation according to our formula standard for the convenience of comparison and uniformity. [b] "ND" means no valid data can be obtained from the literature. [c] We selected the data with cycling performance (>10 cycles) for the comparison and excluded the data with only rate performance and without cycling performance.

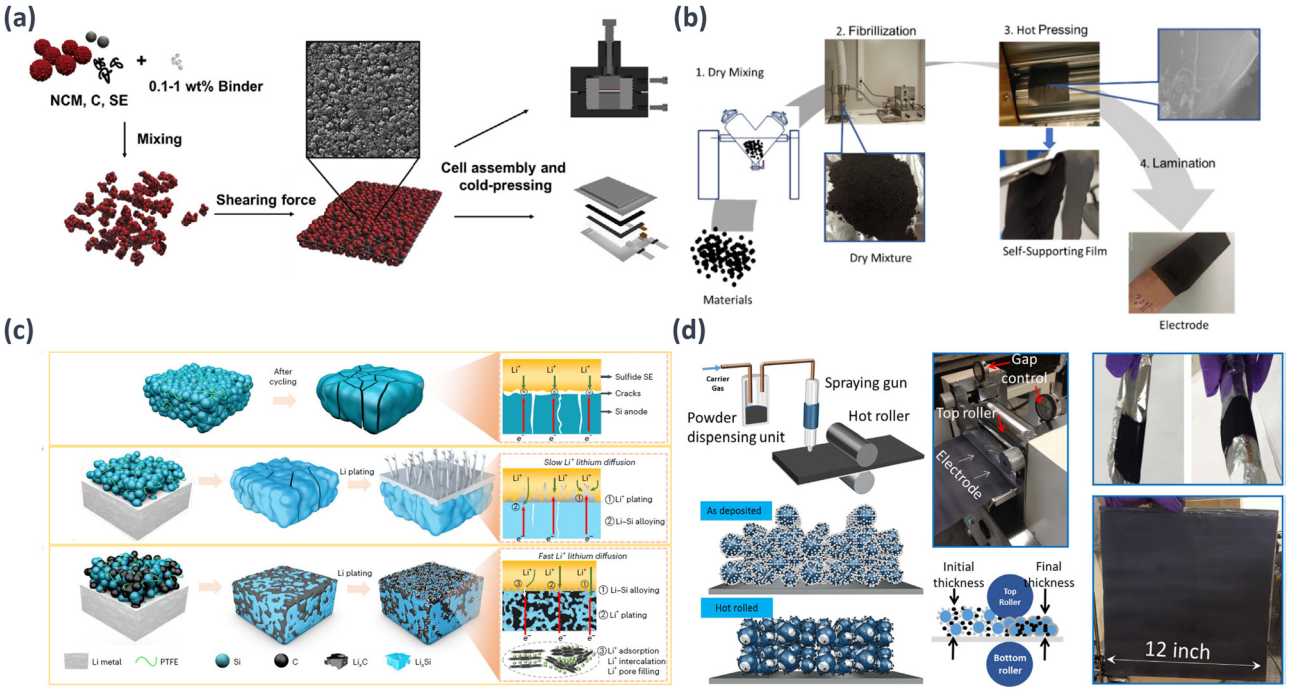

Fig. 8 Schematic examples of the dry fabrication process in: (a) dry premixing of NCM, carbon, SE, and PTFE binder followed by shearing force induced film formation.[128] (b) Solvent-free graphite anode fabrication.[129] (c) Mechanisms for Si, LiSi and LiSH46 anodes in ASSBs.[130] (d) Dry Painted Battery Concept; Manufacturing system for electrodes fabricated through a dry particle painting process. It includes a 3D representation of a dry painted electrode before thermal activation; 3D representation of a dry painted electrode after hot rolling and thermal activation. The configuration of the hot roller and dry painted electrodes on aluminum foils is illustrated.[131]

solid-state batteries differ from conventional LIB electrodes as they need to incorporate solid electrolytes, making their fabrication challenging. Specifically, careful selection of solvents and binders is necessary, and choosing manufacturing methods like dry processing, wet processing, and infiltration is also essential. Table 3 lists details of cell performance such as capacity, C-rate, and cycling performance.[128] This review introduces papers on electrode fabrication methods crucial for the commercialization of all solid-state batteries.

3.1. Dry fabrication

A solvent-free dry manufacturing method can be used to produce electrodes for solid-state batteries. The conventional powder-type electrode fabrication method using hand mixing is limited to laboratory-scale performance, and scaling up to large commercial production has not been feasible. Recently, several research groups have conducted studies on the fabrication of large-area solid-state battery electrodes without using solvents. This solvent-free dry manufacturing approach is suitable for creating thick electrodes with high loading values because it eliminates side reactions caused by interactions with solvents and is well suited for achieving large-area production.

The utilization of polymeric binders in sheet-type cathodes can restrict the ionic conductivity and hinder appropriate electrical interaction with the electrode material. Hippauf *et al.* proposed a solvent-free dry film technique to address these challenges, in which slurry-based binders were substituted with fibrous PTFE binders.[129] Remarkably, binder reduction levels reached as low as 0.1 wt%. They successfully produced a self-supporting NCM sheet featuring a substantial areal loading of 6.5 mA h cm^{-2}, demonstrating a comparable rate performance to the binder-free electrode. Consequently, the solvent-free dry film technique enhanced the performance of sheet-type cathode electrodes and streamlined the battery manufacturing process, offering a promising and simplified strategy, as shown in Fig. 8(a).

Zhang *et al.* conducted a study utilizing a solvent-free dry mixing technique to harness the adhesive properties of PTFE and PVDF and create anode electrodes using carbon materials.[130] The solvent-free electrodes demonstrated remarkable stability for both the hard and soft carbon anodes throughout the charge and discharge cycles. Even at a high loading of 10.7 mg cm^{-2}, the solvent-free hard carbon electrode exhibited a cycling performance comparable to that of conventional slurry casting electrodes. Additionally, $LiNi_{0.5}Co_{0.2}Mn_{0.3}O_2$ displayed an impressive 90% capacity retention after 120 cycles at 1/3C (Fig. 8(b)). Yan *et al.* proposed a high-performance all-solid-state LIB with a stabilized lithium–silicon alloy anode embedded in a robust carbon matrix.[131] By using hard carbon to stabilize the lithium–silicon alloy anode, effective suppression of lithium dendrite growth was achieved, addressing the challenges related to volume changes during lithium insertion and extraction cycles. The assembly of the ASSBs incorporated a LiSH46 anode and an LCO cathode using a dry electrode manufacturing process with a PTFE binder. These ASSBs exhibited the capability to endure 30 000 cycles at a current

density of 20C (14.64 mA cm^{-2}) while maintaining an areal capacity of 0.7 mA h cm^{-2}. Furthermore, the LiSH46 anode contributed to NMC811-based ASSBs achieving 5000 cycles with a loading of 5.86 mA h cm^{-2} and a current density of 5.86 mA cm^{-2}. Impressively, a remarkably high discharge current density of 155.3 mA cm^{-2} was attained along with an NMC811 loading of 6 mA h cm^{-2}. Ultimately, by utilizing the loading of a 20 mA h cm^{-2} NMC811|LiSH46 full cell, ASSBs with a cell-level energy density of 263 W h kg^{-1} and an areal capacity of 16.92 mA h cm^{-2} were successfully obtained. A dry electrode with a PTFE binder can be applied to both the anode and cathode, making it suitable for creating high-loading composite electrodes. Consequently, solid-state batteries employing dry composite electrodes have the potential to achieve high energy densities (Fig. 8(c)).

Instead of utilizing a solvent-reliant method, Ludwig *et al.* proposed a solvent-free dry powder painting technique, in which LCO and NMC electrodes were deposited using completely dry electrode particles onto a current collector *via* an electrostatic spraying system.[132] This innovative dry painting approach is projected to reduce labor, capital equipment, and facility space requirements by approximately 15% in battery manufacturing. Moreover, by eliminating solvent-related steps, both the production time and associated costs were decreased. The bond strength of the electrode achieved a significant improvement, measuring 148.8 kPa compared with the slurry-cast electrode's 84.3 kPa. Electrochemical testing revealed that the new electrode outperformed the conventional slurry-treated electrode owing to variations in binder distribution (Fig. 8(d)).

3.2. Wet-slurry fabrication

The electrode manufacturing method commonly used for traditional commercial LIBs is the wet process of slurry casting. The wet-slurry fabrication process offers significant advantages for mass production. However, solid-state batteries require the integration of SEs into the electrode, and the selection of solvents is limited because of the strong reactivity of SEs with polar solvents. Therefore, solvents with relatively low polarity or non-polarity should be used. Consequently, various research groups have recently conducted studies to explore the optimal solvents and investigate binders with ion conductivity, as solid-state batteries must overcome these challenges for successful electrode fabrication. Oh *et al.* introduced a novel strategic approach by combining sulfide SEs with thermally stable and slurry-fabricated dry polymer electrolyte (DPE) binders to prevent the nucleophilic attack caused by polar functional groups present in common organic solvents.[133] The chosen binder, suitable for slurry formation, can be employed with ester solvents containing bulky alkyl groups, such as benzyl acetate (BA), allowing the dissolution of both polymers and lithium salts. Notably, these DPE-type binders remained intact when in contact with susceptible sulfide SEs. By adopting DPE-type binders such as NA-LiTFSI, the utilization of electrode active materials for NCM increased from 158 to 170 mA h g^{-1} and that

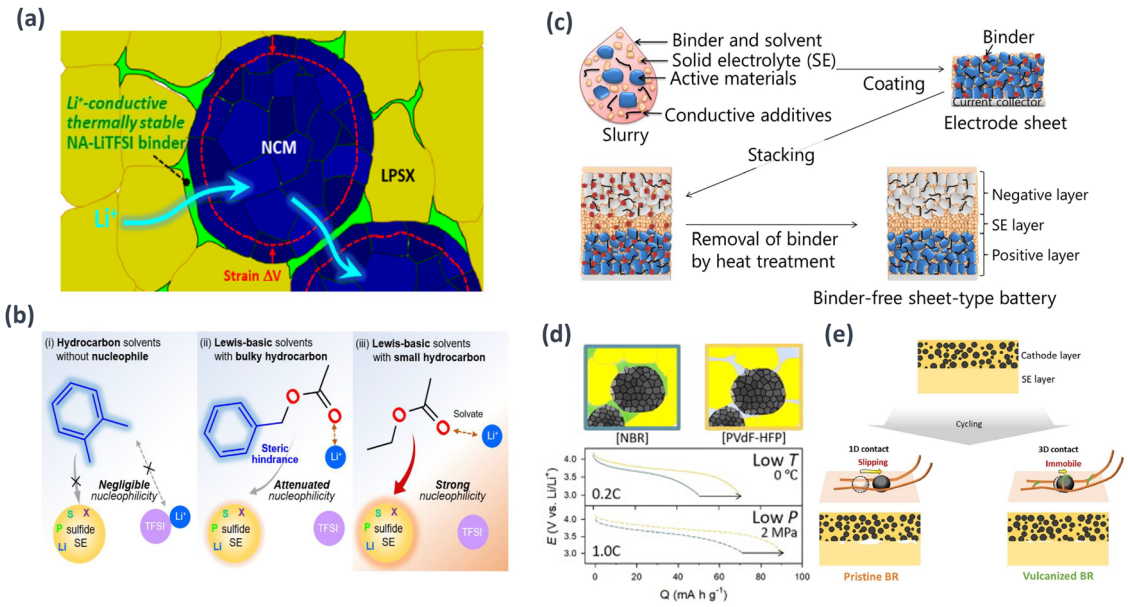

Fig. 9 Schematic examples of the wet-slurry fabrication process in: (a) Microstructure of NCM composite electrodes fabricated using DPE-type binders like NA-LiTFSI, which provide undisturbed interfacial ionic transport pathways without suffering thermal degradation even when the electrode active materials of NCM undergo volumetric changes. (b) Reactivity with LPSX for (i) hydrocarbon solvents (*e.g.*, *o*-xylene), (ii) Lewis-basic solvents with bulky hydrocarbons (*e.g.*, BA), and (iii) Lewis-basic solvents with small hydrocarbons (*e.g.*, EA). Notably Lewis-basic solvents with bulky hydrocarbons, such as BA, do not interact with LPSX due to the steric hindrance from the bulky benzyl group, and they can dissolve Li salts due to the polar acetate group.[132] (c) Strategy for creating binder-free sheet-type ASSLBs.[133] (d) Polymeric binders, NBR and PVdF-HFP, and discharge voltage profiles at 0 °C and 2 Mpa.[134] (e) Electrochemo-mechanical effects within NCM electrodes using pristine and vulcanized BR upon cycling. Different responses against mechanical forces for the linear (pristine, left) and crosslinked (right) BR, and the resulting different degrees of degradation are illustrated.[135]

for graphite increased from 265 to 320 mA h g^{-1}. Furthermore, these DPE-type binders exhibited sustained functionality even under rigorous 70 °C high-temperature testing conditions (Fig. 9(a) and (b)).

Yamamoto *et al.* presented a noteworthy approach involving binder-free sheet-type ASSBs to overcome the challenges caused by the use of binders in sulfide-based electrolytes.[134] A volatile poly(propylene carbonate)-based binder and anisole enabled the fabrication of electrodes and SE sheets. This approach addresses the conflicting requirements by solvating the binder and maintaining the properties of the SE. The resulting full cell, consisting of a binder-free SE sheet and NCM cathode, achieved a cell-based energy density of 115 W h kg^{-1}. This value was calculated from the initial discharge capacity (116 mA h g^{-1}), average discharge voltage (3.51 V), and cell weight without the current collector (PE 16.38 mg, SE 10.93 mg, NE, 16.89 mg). This provided insights into cell performance and energy density enhancement while eliminating the drawbacks of binder usage in ASSBs (Fig. 9(c)).

The reactivity of sulfide SEs with polar solvents can limit the range of suitable slurry-processing solvents and, consequently, restrict the scope of polymer binder utilization. To address this problem, Kim *et al.* proposed a slurry fabrication approach using co-solvents and lithium salts to introduce Li^+-conductive dry-polymer-electrolyte-based binders into all-solid-state lithium batteries.[135] Specifically, DBM and HB synergistically dissolved NBR and LiTFSI while effectively controlling the polymer dispersion within the slurry protocol. The resulting pellet-type NCM/Gr full cells fabricated with PVDF-HFP electrodes demonstrated an initial discharge capacity of 160 mA h g_{NCM}^{-1} at 0.2C. Notably,

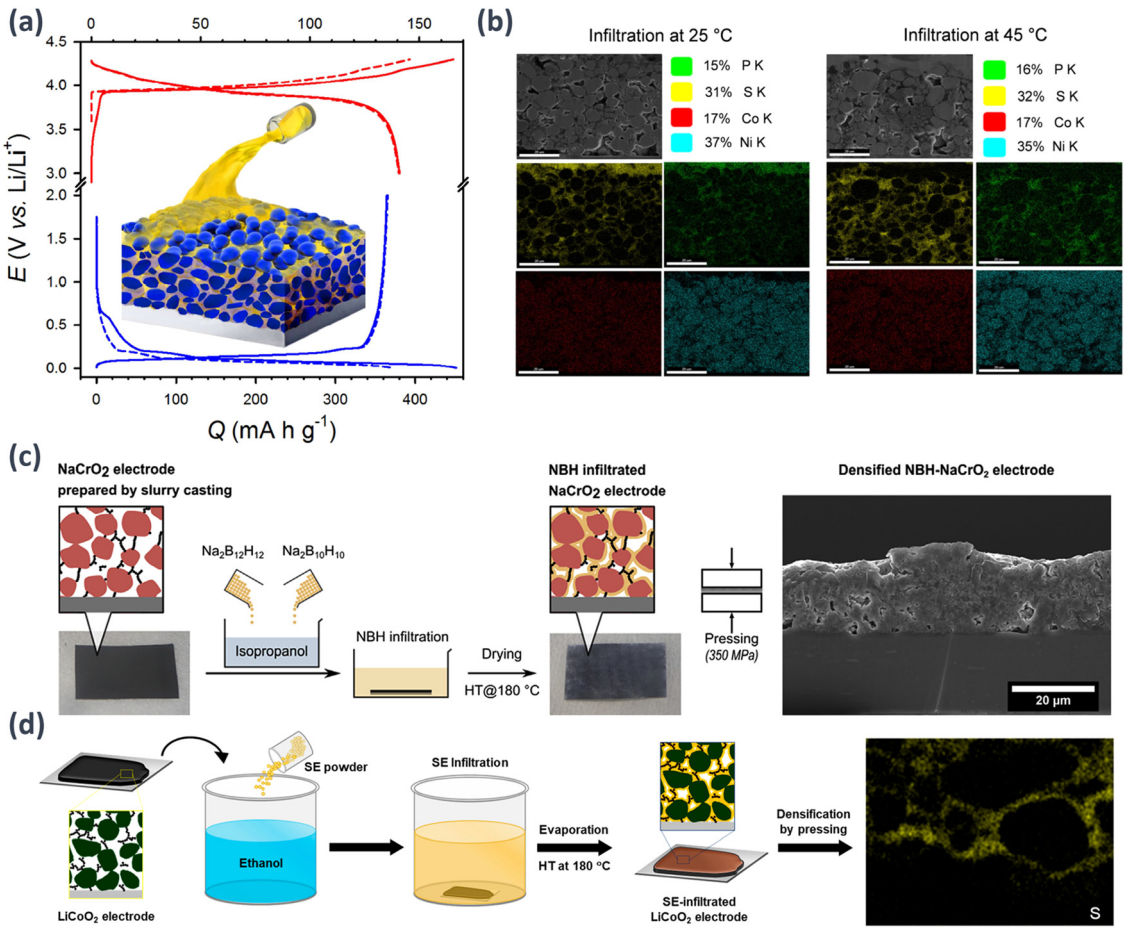

Fig. 10 (a) Schematic of a scalable electrode fabricated by infiltrating traditional LIB electrodes with solution-processable SEs and the charge–discharge profile.[138] Reprinted (adapted) with permission from ref. 138, Copyright 2017 American Chemical Society. (b) Cross-sectional field emission scanning electron microscopy (FE-SEM) images of NCM622-based composite electrodes infiltrated with LPSCl, along with their respective energy dispersive X-ray spectroscopy (EDXS) elemental maps, were obtained. The cathode electrodes were prepared by the SE infiltration process at varying temperatures at room and high (45 °C) temperatures. The loading value of the electrodes was ~17.92 mg cm^{-2}. Following the cross-sectional cutting the electrodes using a focused ion beam (FIB), the homogeneous distributions of SE elements (representatively sulfur ions) were analysed and the homogeneous distribution of SE within the electrodes was confirmed when infiltrated at 45 °C.[141] (c) Schematic of the fabrication of $NaCrO_2$ electrodes infiltrated with the $Na_4(B_{12}H_{12})(B_{10}H_{10})$ SE by solution processing. Images of the electrodes prepared by slurry coating and their corresponding schematic cross-sectional images before and after infiltration. PVDF are excluded for simplicity. A cross-sectional SEM image of the densified $Na_4(B_{12}H_{12})(B_{10}H_{10})$–$NaCrO_2$ infiltrated electrode is also shown.[143] (d) Schematic of the infiltration of slurry cast $LiCoO_2$ electrodes with LPGeSI-EtOH solutions.[140] Reprinted (adapted) with permission from ref. 130, Copyright 2020 American Chemical Society.

these cells showed excellent capacity retention (93.2%) even after 200 cycles. Furthermore, pouch-type NCM/Gr all-solid-state lithium batteries assembled without externally applied pressure exhibited a first-cycle discharge capacity of 169 mA h g_{NCM}^{-1} at 0.1C, matching the results observed in pellet-type cells (Fig. 9(d)).

Typically, laboratory-scale pellet-type all-solid-state cells are manufactured with or without polymeric binders. These cells are often evaluated under impractically high external pressures. Kwon *et al.* introduced a scalable approach involving the *in situ* crosslinking of BR using elemental sulfur (vulcanization) during the wet-slurry fabrication of sheet-type electrodes utilizing sulfide SEs.[136] Customized NCM electrodes with vulcanized BR exhibited superior performance compared with those with original BR, even at a low pressure of 2 MPa (first discharge capacities of 165 and 151 mA h g^{-1}, respectively). Notably, NCM/LTO pouch-type full cells, tested without pressure, displayed significant performance enhancement using vulcanized BR (165 *vs.* 150 mA h g^{-1} and 153 *vs.* 121 mA h g^{-1} at 0.05C and 0.2C, respectively). This protocol demonstrates its feasibility and potential for improving cell performance without unrealistically high pressure, as shown in Fig. 9(e).

3.3. Infiltration fabrication processes

In the manufacturing of cathodes containing sulfide-based SEs such as LPSCl, nonpolar solvents or solvents with low polarity are commonly used considering the reactivity of the SE. However, research on the synthesis of SEs using weakly polar solvents has also been reported. For example, (LiI)–Li_4SnS_4 using methanol (MeOH),[137] $Li_{6-x}PS_{5-x}[Cl,Br]_x$ or $Li_{6+x}P_{1-x}M_xS_5I$ (M = Ge, Sn) using ethanol (EtOH),[138–142] Na_3SbS_4 using water or MeOH,[143] and $Na_4(B_{12}H_{12})(B_{10}H_{10})$ using isopropanol.[144] In the solution process, SEs are completely dissolved to create uniform solutions. The initial SEs are then recrystallized by precipitation under vacuum and subsequent heat treatment. This solution-based approach introduces innovative fabrication methods for sheet-type electrodes in ASSBs while also enhancing the advantage of intimate ionic contact.[139–143]

An LPSCl solution with EtOH as a base was used to infiltrate sheet-type conventional porous LIB electrodes. These electrodes consist of an active material with PVDF as the binder and *N*-methyl-2-pyrrolidone as the solvent. Composite electrodes were fabricated using a sequential process involving drying and subsequent heat treatment. The LPSCl-infiltrated LCO and Gr electrodes achieved high reversible capacities of 141 mA h g^{-1} and 364 mA h g^{-1}, respectively, at 0.1C and 30 °C (Fig. 10(a)).[139] By controlling the temperature of the SE solution during the infiltration process, we observed high discharge capacities even in electrodes with a high loading level (approximately 17 mg cm^{-2}). This demonstrates the potential for achieving a high energy density through the infiltration process (Fig. 10(b)).[142] Moreover, the potential of the infiltration process is not limited to the cathode in LIB systems. This approach can also be effectively extended to Si anodes.[140] Also, this infiltration process can be adapted for applications in Na-ion batteries utilizing closo-borate-based electrolytes, particularly $Na_4(B_{12}H_{12})(B_{10}H_{10})$ (Fig. 10(c)).[143]

Song *et al.* successfully developed iodine-based lithium argyrodites with LPSI, LPGeSI, and LPSnSI compositions and high Li^+-ion conductivity through solution processing.[141] Among them, $Li_{6.5}P_{0.5}Ge_{0.5}S_5I$ exhibited the highest Li^+-ion conductivity of 0.54 mS cm^{-1} at 30 °C. In addition, they demonstrated the excellent electrochemical performance of $LiCoO_2$ electrodes infiltrated with LPGeSI, showing promising potential for practical applications (Fig. 10(d)).

The mentioned promising technologies are expected to contribute to the future commercialization of ASSB electrodes. Utilizing the existing equipment from LIB roll-to-roll processes offers economic advantages. The simplified process facilitates close contact between the electrode material and the SE, resulting in excellent electrochemical performance with a relatively small amount of SE. However, challenges remain, including performance degradation caused by solvent-related side reactions and the need for process optimization to ensure uniform infiltration. These factors should be considered for optimal results.

4. Applications of solid electrolytes beyond ASSBs

Although LIBs have revolutionized portable electronics, their limitations in terms of safety, energy density, and capacity have prompted researchers to seek alternative battery technologies. Lithium–sulfur, sodium-ion, and magnesium-ion batteries with SEs have been explored to address these challenges and pave the way for a more sustainable and energy-dense future. Because the lithium–sulfur system offers exceptionally high theoretical energy densities owing to the high capacity of sulfur as a cathode material,[145–147] a promising avenue is the development of all-solid-state lithium–sulfur batteries (ASSLSB). Additionally, all-solid-state sodium-ion batteries (ASSSIB) and all-solid-state magnesium-ion batteries (ASSMIB) have been studied as alternatives, leveraging more abundant raw materials than lithium.[148–153] SEs are being explored to enhance the safety of these batteries by replacing the flammable liquid electrolytes used in traditional

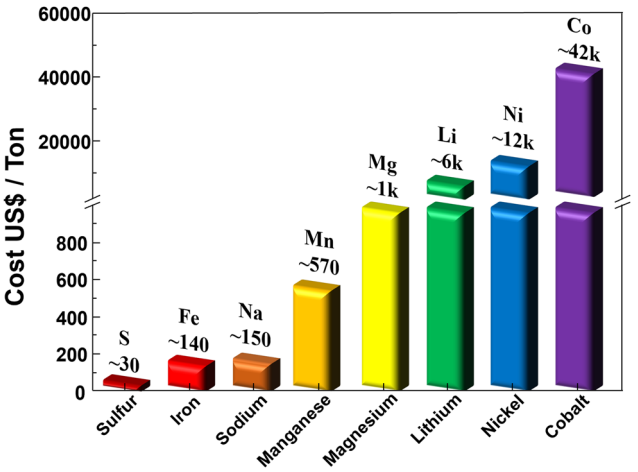

Fig. 11 Comparison of manufacturing costs of S, Fe, Na, Mn, Li, Ni, and Co.

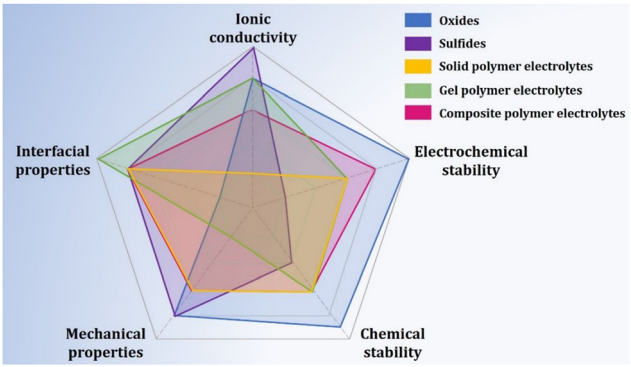

Fig. 12 Comparison of the performance of SSEs with oxide, sulfide, and polymer systems. Reprinted with permission from ref. 153. Copyright 2020 American Chemical Society.

LIBs. In particular, these alternative electrochemical energy storage devices have low manufacturing costs compared to conventional LIBs, as shown in Fig. 11.

4.1. ASSBs with sulfur

Sulfur has many advantages as a cathode material for next-generation lithium secondary batteries, such as its low cost, eco-friendliness, and abundance. It also offers higher volumetric and gravimetric energy densities of 2800 W h L^{-1} and 2500 W h kg^{-1}, respectively, compared with conventional cathode materials.[54] Therefore, sulfur has attracted significant interest as an alternative to traditional cathode materials. However, the commercialization of lithium–sulfur batteries is difficult because of critical issues involving the dissolution of lithium polysulfide (LiPS) and growth of lithium dendrites on the lithium anode surface during the charge and discharge processes. To address this issue, the substitution of conventional liquid-state electrolytes with SSEs is a viable option to solve the aforementioned critical problems and facilitate commercialization, as they can suppress both LiPS dissolution and lithium dendrite growth. This section focuses on recent advances in ASSLSBs using various types of SSEs with sulfur cathodes.

Pan *et al.* reviewed ASSLSBs and outlined five prerequisite conditions for SSEs in ASSLSBs: (1) favorable ionic conductivity of SSEs exceeding 10^{-4} S cm^{-1} with low electron conductivity, (2) good lithium-ion transference number, (3) good chemical and electrochemical stabilities when paired with lithium metal anodes and sulfur cathodes, (4) low interfacial resistance, and (5) eco-friendliness and nontoxicity when in contact with both cathodes and anodes.[154] Fig. 12 shows radar charts displaying the performance of various types of SSEs for ASSLSBs. SSEs can be categorized into three groups: (1) sulfides, (2) oxides, and (3) polymers.

Sulfide SSEs for ASSLSBs have good ionic conductivity ($\sim 10^{-3}$ S cm^{-1} at room temperature) and are mechanically soft compared with oxide-system SSEs. However, the instability of sulfide-system SSEs against lithium dendrite growth during cycling remains a challenge for the commercialization of ASSLSBs. To address this, Wan *et al.* synthesized lithophilic and lithiophobic interlayers between $Li_{10}GeP_2S_{12}$ (LGPS) and lithium metal (Fig. 13(a)–(c)).[155] Through this approach, they effectively suppressed lithium dendrite growth during cycling by forming a bifunctional Li_xMg/LiF/polymer lithiophilic/lithiophobic SE interface between the lithium metal anode and LGPS, resulting in the improved cyclability of ASSLSBs (discharge capacity of 400.6 mA h g^{-1} at the 120th cycle). Yi *et al.* reported the synthesis of a $Li_{10}SnP_2S_{12}$ SSE through high-energy ball milling and heat treatment (Fig. 13(d)–(f)).[156] It exhibits a high ionic conductivity of 3.2×10^{-3} S cm^{-1} at room temperature. S-C-$Li_{10}SnP_2S_{12}$ was used as the cathode and lithium–indium foil as the anode to assemble an electrochemical cell. The S-C-$Li_{10}SnP_2S_{12}$/$Li_{10}SnP_2S_{12}$ SSE/Li–In cell showed a discharge capacity of 1601.7 mA h g^{-1} at the 1st cycle. After the 50th cycle, the cell delivered a discharge capacity of 1180.3 mA h g^{-1} with a superior coulombic efficiency of approximately 100% for 50 cycles.

Oxide SSEs have also been widely studied because of their strong mechanical and chemical stabilities in air, making them suitable for commercializing ASSLSBs. Pervez *et al.* successfully suppressed lithium dendrite growth during cycling and reduced the interface resistance between the lithium metal anode and the SSE using an LLZO SSE, resulting in improved cyclability.[157] Kim *et al.* synthesized a polymer-based SSE for ASSLSBs using UV curing.[158] The UV polymer-based ASSLSBs exhibited good flexibility and a long lifespan, as shown in Fig. 13(g). In addition, they assembled bipolar stack cells for high-voltage ASSLSBs with favorable thermal stability and foldability (Fig. 13(h)). Hybrid SSEs have also been developed using a combination of inorganic and polymeric materials to enhance the electrochemical performance of ASSLSBs. Li *et al.* reported a thio-LiSICON/polymer ($Li_{3.25}Ge_{0.25}P_{0.75}S_4$/PEO) composite electrolyte that reduced internal resistance between the SSE and electrodes.[159] This composite electrolyte resulted in excellent charge and discharge performances, with discharge capacities of 1183 mA h g^{-1} and 719 mA h g^{-1} at 0.2 C-rate and 0.5 C-rate, respectively.

4.2. ASSBs with sodium

Compared with lithium, which is widely used in rechargeable batteries, sodium is more abundant and cost-effective. This makes sodium-ion batteries (SIB) an attractive option for applications that require a large amount of energy storage capacity, such as renewable energy integration, grid stabilization, and load leveling.[160–162] SIBs can potentially offer a lower cost per unit of stored energy, which is essential for making large-scale energy storage solutions economically viable. Furthermore, the development of advanced sodium-ion battery technologies and materials is ongoing with the aim of improving their performance in terms of energy density, cycle life, and safety. Researchers are working to optimize the chemistry and design of SIBs to make them more competitive with other energy storage technologies for commercialization.[163,164] As SSEs have attracted attention because of their lack of liquid electrolyte leakage, good thermal stability, and low flammability, ASSSIBs have been widely studied. Fig. 14(a) and (b) show schematic illustrations of ASSSIBs and flexible ASSSIBs, respectively.[165]

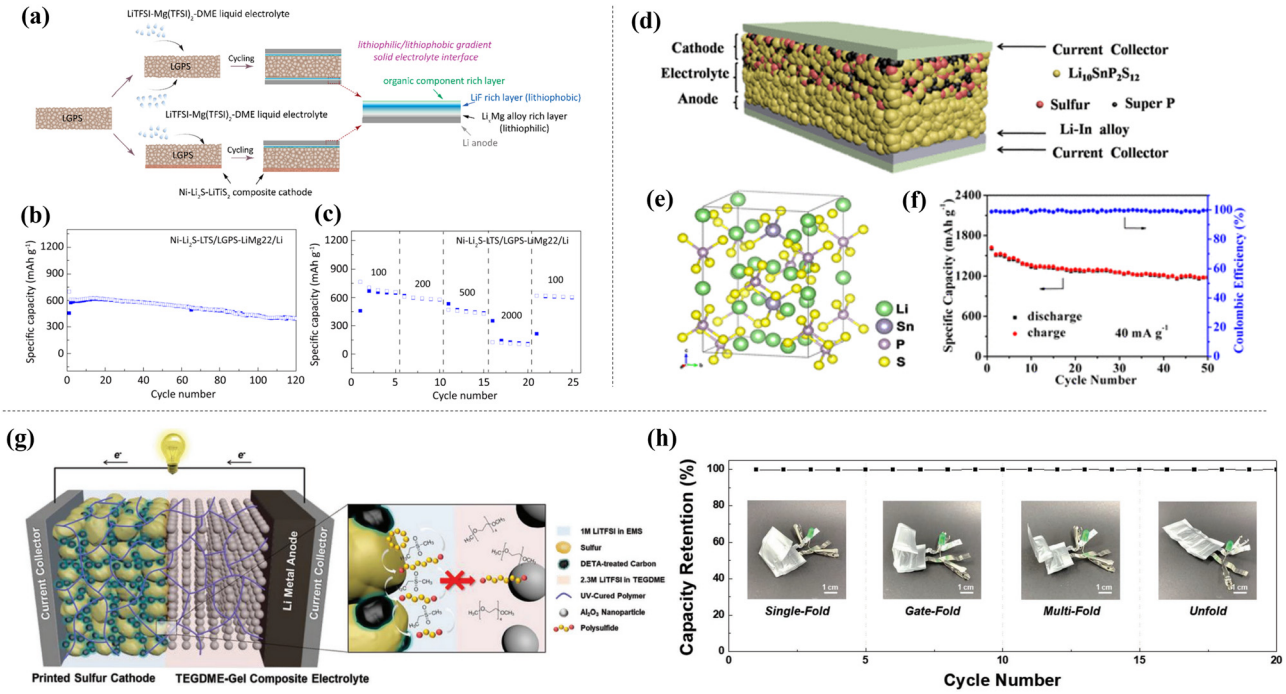

Fig. 13 (a) Illustration of lithiophilic–lithiophobic SSE, (b) cyclability for 120 cycles, and (c) rate-performance at various C-rate conditions.[154] Reprinted with permission from ref. 154. Copyright 2021 American Chemical Society. (d) Structure of ASSLSBs with $Li_{10}SnP_2S_{12}$ SSE, (e) crystal structure of $Li_{10}SnP_2S_{12}$, (f) cyclability with coulombic efficiency of the test cell for 50 cycles.[156] Reprinted with permission from ref. 156. Copyright 2019 American Chemical Society. (g) Schematic illumination of UV cured ASSLSBs, and (h) folding test of pouch type cell for 25 cycles.[157] Reproduced with permission of John Wiley and Sons.

Matios *et al.* synthesized ASSSIBs using an ultrathin graphene layer and NASICON (G-NASICON) to enhance the interfacial contact between the Na metal anode and the SSE, resulting in Na plating/stripping cycling stability (Fig. 14(c) and (d)).[166] In addition, Na dendrite growth was suppressed using a G-NASICON ceramic separator, as shown in Fig. 14(e) and (f). Flexible ASSSIBs were reported by Zhao *et al.* in 2022 using a flexible carbon cloth and polymer-based SSEs. The flexible ASSSIBs exhibited excellent cyclability with good discharge capacity (1.4 mA h g^{-1} for 2000 cycles) and capacity retention (77% at 5 C-rate rate). Remarkably, the flexible ASSSIBs pouch cell continued to operate after the cutting test.[167]

4.3. ASSBs with magnesium

Magnesium-ion batteries (MIB) have attracted attention in recent decades because of their high gravimetric (2046 mA h g^{-1}) and volumetric (3833 mA h cm^{-3}) energy densities, low manufacturing cost, low redox potential (−2.36 V *vs.* SHE), abundance, and eco-friendliness.[168–170] Despite these advantages, MIBs face commercialization challenges because of their poor cycling stability,

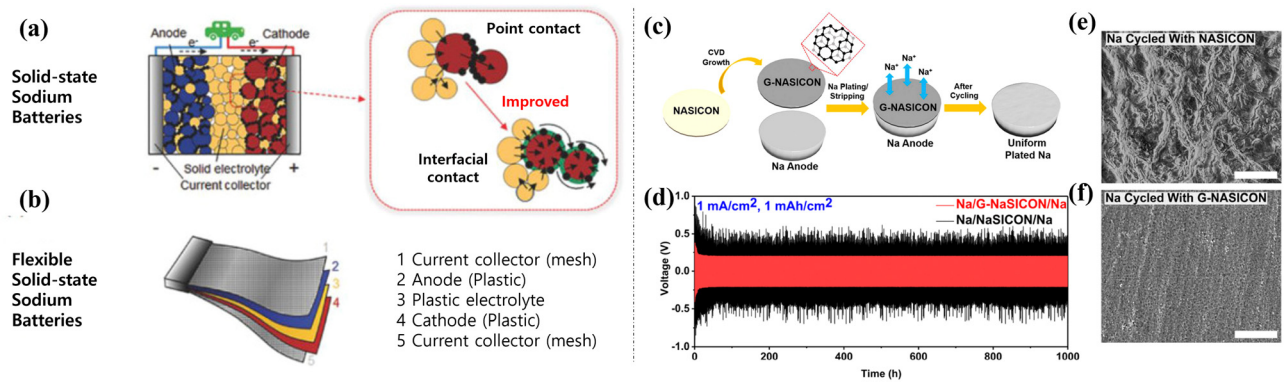

Fig. 14 Illustration of (a) solid-state sodium batteries and (b) flexible solid-state sodium batteries. Reprinted with permission from ref. 164. Copyright 2021 American Chemical Society. (c) ASSSIBs prepared with ultrathin graphene layer-NASICON. (d) Na stripping/plating cycling performances with (e) graphene layer-NASICON and (f) conventional NASICON and their surface morphologies. Reprinted with permission from ref. 165. Copyright 2019 American Chemical Society.

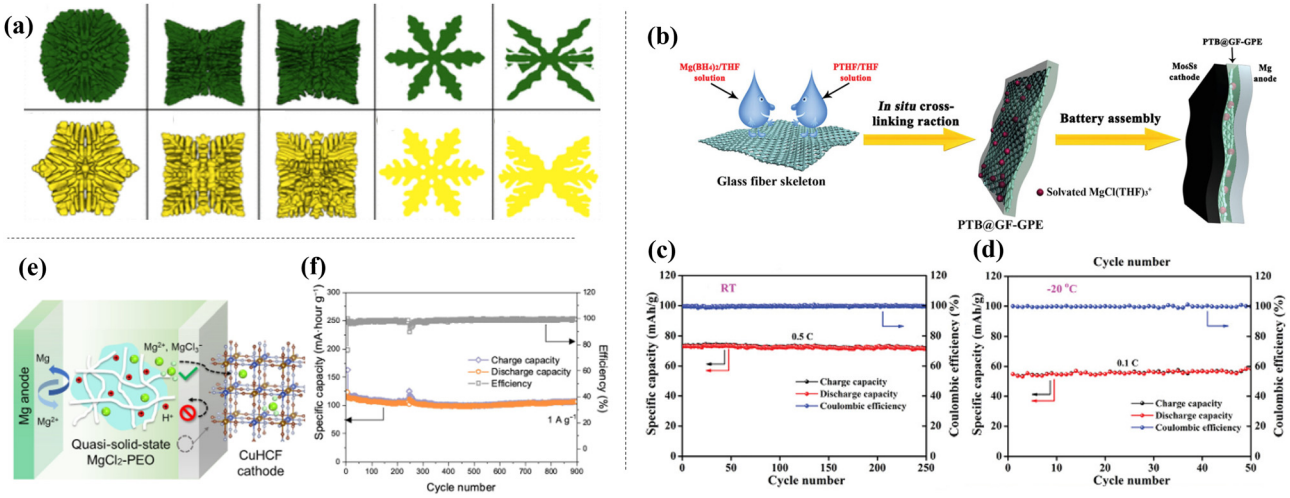

Fig. 15 (a) Various shapes of Mg dendrite growth patterns,[170] reprinted with permission from ref. 170. Copyright 2022 American Chemical Society. (b) Schematic illustration of crosslinked polymer based SSE by *in situ* cross-linking reaction, cycle performance at (c) room temperature and (d) −20 °C.[171] Reproduced with permission of John Wiley and Sons. (e) Illustration of ASSMIBs with SSE synthesized using PEO with aqueous-based electrolyte and (f) its cyclability for 900 cycles.[172]

sluggish kinetics, and magnesium dendrite growth during cycling (Fig. 15(a)).[171] In particular, magnesium dendrite growth on the magnesium anode surface is a critical problem because it causes short circuits between the cathode and anode, resulting in thermal runaway of the cell. Therefore, employing an all-SSE is a good option for suppressing the growth of Mg dendrites. Du *et al.* have reported a crosslinked polymer-based SSE for MIBs that exhibits good electrochemical performances not only at room temperature but also for wide temperature ranges (−20 to 60 °C).[172] A cross-linked polymer-based SSE was synthesized *via* an *in situ* cross-linking reaction using magnesium borohydride and hydroxyl-terminated polytetrahydrofuran. The cell exhibited a discharge capacity of 72 mA h g^{-1} and 58 mA h g^{-1} at room temperature and −20 °C (Fig. 15(c) and (d)), making it a potential solution for short-circuits. To improve the cyclability of ASSMIBs, Leong *et al.* fabricated and tested ASSMIBs using PEO in an aqueous electrolyte.[173] The SSE showed an excellent chemical stability at high voltage (2.6 to 2.0 V plateau). Furthermore, the cell displayed a superior cyclability over 900 cycles with a good capacity retention of 88% owing to the anchoring ability of hydrogen bonds in the PEO structure.

5. Conclusions and perspectives

This review provided a comprehensive examination of the challenges and emerging research trends in the field of ASSBs, with the ultimate goal of facilitating their commercialization, going beyond the discussion of the advancements in ASSBs and exploring the potential applications of all-solid-state electrolytes in other next-generation battery technologies. The key contents of this article are organized into three main themes. First, it addresses the crucial considerations for the successful commercialization of ASSBs and highlights the key challenges that need to be overcome. Second, this review delves into the strategies that researchers have employed to address these challenges, providing insights into the latest developments in this field. Finally, this article explores alternative applications of SEs beyond ASSBs, shedding light on their potential use in other battery technologies.

In addition to the factors mentioned in this review, several other considerations must be addressed for the practical application of next-generation batteries in EVs. Many recent studies have focused on showcasing battery performance at high temperatures and maintaining the contact area under high-pressure conditions. However, for practical applications, ASSBs must demonstrate excellent performance at room temperature and low operating pressures, particularly in pouch-cell-type configurations, rather than just in high-pressure press cell types. This poses a significant challenge that requires further research and improvement. Furthermore, advancements in anode technology are essential to ensure the successful commercialization of solid-state batteries. Lithium metal is a leading candidate for ASSB anodes, and research on lithium-free anodes is actively ongoing.[174,175] Additionally, research on low-reactivity silicon anodes is in progress, with studies reporting on their exceptional performance using additive-free, electrolyte-free, and void-free silicon wafer electrodes.[176]

Overall, this comprehensive review serves as a valuable resource for researchers and industry professionals seeking guidance and solutions for the commercialization of ASSBs. By covering a wide range of topics, from challenges to strategies and alternative applications, this review offers important insights and directions for advancing the field and realizing the full potential of ASSBs.

Author contributions

J. Sung: investigation, writing – original draft, writing – review & editing. J. Heo: investigation, writing – original draft, writing –

review & editing. D.-H. Kim: investigation, writing – review & editing. S. Jo: visualization, writing – review & editing. Y.-C. Ha: validation, writing - review & editing. D. Kim: validation, writing – review & editing. S. Ahn: funding acquisition, validation, visualization, writing – review & editing. J.-W. Park: funding acquisition, validation, visualization, writing – review & editing.

Conflicts of interest

There are no conflicts of interest to declare.

Acknowledgements

This study was supported by the Ministry of Trade, Industry and Energy (MOTIE, Korea) (No. 20014581, 20007045, and 00254457), by Korea Electrotechnology Research Institute (KERI) (No. 24A01017), and by the National Research Foundation of Korea (NRF) grant funded by the Korea government (MSIT, Korea) (No. NRF-2021R1G1A1094175).

References

1 B. Scrosati and J. Garche, Lithium batteries: Status, prospects and future, *J. Power Sources*, 2010, **195**, 2419–2430.
2 G. Zhou, F. Li and H.-M. Cheng, Progress in flexible lithium batteries and future prospects, *Energy Environ. Sci.*, 2014, **7**, 1307–1338.
3 M. S. Whittingham, Lithium Batteries and Cathode Materials, *Chem. Rev.*, 2004, **104**, 4271–4302.
4 Y. Nishi, Lithium ion secondary batteries; past 10 years and the future, *J. Power Sources*, 2001, **100**, 101–106.
5 K. Brandt, Historical development of secondary lithium batteries, *Solid State Ionics*, 1994, **69**, 173–183.
6 G. E. Blomgren, The Development and Future of Lithium Ion Batteries, *J. Electrochem. Soc.*, 2017, **164**, A5019.
7 X. Zeng, M. Li, D. Abd El-Hady, W. Alshitari, A. S. Al-Bogami, J. Lu and K. Amine, Commercialization of Lithium Battery Technologies for Electric Vehicles, *Adv. Energy Mater.*, 2019, **9**, 1900161.
8 J. Speirs, M. Contestabile, Y. Houari and R. Gross, The future of lithium availability for electric vehicle batteries, *Renewable Sustainable Energy Rev.*, 2014, **35**, 183–193.
9 K. Tamura and T. Horiba, Large-scale development of lithium batteries for electric vehicles and electric power storage applications, *J. Power Sources*, 1999, **81–82**, 156–161.
10 Q. Wang, B. Jiang, B. Li and Y. Yan, A critical review of thermal management models and solutions of lithium-ion batteries for the development of pure electric vehicles, *Renewable Sustainable Energy Rev.*, 2016, **64**, 106–128.
11 A. Burke and M. Miller, The power capability of ultracapacitors and lithium batteries for electric and hybrid vehicle applications, *J. Power Sources*, 2011, **196**, 514–522.
12 C. Zhang, Y.-L. Wei, P.-F. Cao and M.-C. Lin, Energy storage system: Current studies on batteries and power condition system, *Renewable Sustainable Energy Rev.*, 2018, **82**, 3091–3106.
13 W. Tang, Y. Zhu, Y. Hou, L. Liu, Y. Wu, K. P. Loh, H. Zhang and K. Zhu, Aqueous rechargeable lithium batteries as an energy storage system of superfast charging, *Energy Environ. Sci.*, 2013, **6**, 2093–2104.
14 X. Liang, J. Yun, Y. Wang, H. Xiang, Y. Sun, Y. Feng and Y. Yu, A new high-capacity and safe energy storage system: lithium-ion sulfur batteries, *Nanoscale*, 2019, **11**, 19140–19157.
15 T. Chen, Y. Jin, H. Lv, A. Yang, M. Liu, B. Chen, Y. Xie and Q. Chen, Applications of Lithium-Ion Batteries in Grid-Scale Energy Storage Systems, *Trans. Tianjin Univ.*, 2020, **26**, 208–217.
16 D. H. Doughty, P. C. Butler, A. A. Akhil, N. H. Clark and J. D. Boyes, Batteries for Large-Scale Stationary Electrical Energy Storage, *Electrochem. Soc. Interface*, 2010, **19**, 49.
17 W. Li, I. Demir, D. Cao, D. Jöst, F. Ringbeck, M. Junker and D. U. Sauer, Data-driven systematic parameter identification of an electrochemical model for lithium-ion batteries with artificial intelligence, *Energy Storage Materials*, 2022, **44**, 557–570.
18 R. P. Cunha, T. Lombardo, E. N. Primo and A. A. Franco, Artificial Intelligence Investigation of NMC Cathode Manufacturing Parameters Interdependencies, *Batteries Supercaps*, 2020, **3**, 60–67.
19 M.-F. Ng, J. Zhao, Q. Yan, G. J. Conduit and Z. W. Seh, Predicting the state of charge and health of batteries using data-driven machine learning, *Nat. Mach. Intell.*, 2020, **2**, 161–170.
20 M. Zheng, H. Salim, T. Liu, R. A. Stewart, J. Lu and S. Zhang, Intelligence-assisted predesign for the sustainable recycling of lithium-ion batteries and beyond, *Energy Environ. Sci.*, 2021, **14**, 5801–5815.
21 D. H. Barrett and A. Haruna, Artificial intelligence and machine learning for targeted energy storage solutions, Current Opinion in, *Electrochemistry*, 2020, **21**, 160–166.
22 I.-H. Cho, P.-Y. Lee and J.-H. Kim, Analysis of the Effect of the Variable Charging Current Control Method on Cycle Life of Li-ion Batteries, *Energies*, 2019, **12**, 3023.
23 M. Wakihara, Recent developments in lithium ion batteries, *Mater. Sci. Eng., R*, 2001, **33**, 109–134.
24 J.-X. Tang, J.-H. Du, Y. Lin and Q.-S. Jia, Predictive Maintenance of VRLA Batteries in UPS towards Reliable Data Centers, *IFAC-PapersOnLine*, 2020, **53**, 13607–13612.
25 T.-H. Kim, J.-S. Park, S. K. Chang, S. Choi, J. H. Ryu and H.-K. Song, The Current Move of Lithium Ion Batteries Towards the Next Phase, *Adv. Energy Mater.*, 2012, **2**, 860–872.
26 B. Guo, M. Niu, X. Lai and L. Chen, Application research on large-scale battery energy storage system under Global Energy Interconnection framework, *Global Energy Interconnect.*, 2018, **1**, 79–86.
27 A. Manthiram, Materials Challenges and Opportunities of Lithium Ion Batteries, *J. Phys. Chem. Lett.*, 2011, **2**, 176–184.

28 J. B. Goodenough, Rechargeable batteries: challenges old and new, *J. Solid State Electrochem.*, 2012, **16**, 2019–2029.
29 A. Masias, J. Marcicki and W. A. Paxton, Opportunities and Challenges of Lithium Ion Batteries in Automotive Applications, *ACS Energy Lett.*, 2021, **6**, 621–630.
30 R. Zhan, X. Wang, Z. Chen, Z. W. Seh, L. Wang and Y. Sun, Promises and Challenges of the Practical Implementation of Prelithiation in Lithium-Ion Batteries, *Adv. Energy Mater.*, 2021, **11**, 2101565.
31 Y. Chen, Y. Kang, Y. Zhao, L. Wang, J. Liu, Y. Li, Z. Liang, X. He, X. Li, N. Tavajohi and B. Li, A review of lithium-ion battery safety concerns: The issues, strategies, and testing standards, *J. Energy Chem.*, 2021, **59**, 83–99.
32 X. Wu, K. Song, X. Zhang, N. Hu, L. Li, W. Li, L. Zhang and H. Zhang, Safety Issues in Lithium Ion Batteries: Materials and Cell Design, *Front. Energy Res.*, 2019, **7**, 00065.
33 B. Liu, Y. Jia, C. Yuan, L. Wang, X. Gao, S. Yin and J. Xu, Safety issues and mechanisms of lithium-ion battery cell upon mechanical abusive loading: A review, *Energy Storage Mater.*, 2020, **24**, 85–112.
34 F. H. Gandoman, J. Jaguemont, S. Goutam, R. Gopalakrishnan, Y. Firouz, T. Kalogiannis, N. Omar and J. Van Mierlo, Concept of reliability and safety assessment of lithium-ion batteries in electric vehicles: Basics, progress, and challenges, *Appl. Energy*, 2019, **251**, 113343.
35 J. Lin, C. Zeng, Y. Chen, X. Lin, C. Xu and C.-Y. Su, In situ construction of a MOF-derived carbon-encapsulated $LiCoO_2$ heterostructure as a superior cathode for elevated-voltage lithium storage: from experimental to theoretical study, *J. Mater. Chem. A*, 2020, **8**, 6607–6618.
36 D. Miranda, A. Gören, C. M. Costa, M. M. Silva, A. M. Almeida and S. Lanceros-Méndez, Theoretical simulation of the optimal relation between active material, binder and conductive additive for lithium-ion battery cathodes, *Energy*, 2019, **172**, 68–78.
37 J. L. Pimlott, R. J. Street, M. P. Down and C. E. Banks, Electrochemical Overview: A Summary of $ACo_xMn_yNi_zO_2$ and Metal Oxides as Versatile Cathode Materials for Metal-Ion Batteries, *Adv. Funct. Mater.*, 2021, **31**, 2107761.
38 M. J. Lain and E. Kendrick, Understanding the limitations of lithium ion batteries at high rates, *J. Power Sources*, 2021, **493**, 229690.
39 F. Jiang and P. Peng, Elucidating the Performance Limitations of Lithium-ion Batteries due to Species and Charge Transport through Five Characteristic Parameters, *Sci. Rep.*, 2016, **6**, 32639.
40 K. G. Gallagher, S. E. Trask, C. Bauer, T. Woehrle, S. F. Lux, M. Tschech, P. Lamp, B. J. Polzin, S. Ha, B. Long, Q. Wu, W. Lu, D. W. Dees and A. N. Jansen, Optimizing Areal Capacities through Understanding the Limitations of Lithium-Ion Electrodes, *J. Electrochem. Soc.*, 2016, **163**, A138.
41 J.-Y. Hwang, S.-T. Myung and Y.-K. Sun, Sodium-ion batteries: present and future, *Chem. Soc. Rev.*, 2017, **46**, 3529–3614.
42 C. Delmas, Sodium and Sodium-Ion Batteries: 50 Years of Research, *Adv. Energy Mater.*, 2018, **8**, 1703137.
43 C. Vaalma, D. Buchholz, M. Weil and S. Passerini, A cost and resource analysis of sodium-ion batteries, *Nat. Rev. Mater.*, 2018, **3**, 18013.
44 M. D. Slater, D. Kim, E. Lee and C. S. Johnson, Sodium-Ion Batteries, *Adv. Funct. Mater.*, 2013, **23**, 947–958.
45 N. Yabuuchi, K. Kubota, M. Dahbi and S. Komaba, Research Development on Sodium-Ion Batteries, *Chem. Rev.*, 2014, **114**, 11636–11682.
46 R. C. Massé, E. Uchaker and G. Cao, Beyond Li-ion: electrode materials for sodium- and magnesium-ion batteries, Science China, *Materials*, 2015, **58**, 715–766.
47 M. M. Huie, D. C. Bock, E. S. Takeuchi, A. C. Marschilok and K. J. Takeuchi, Cathode materials for magnesium and magnesium-ion based batteries, *Coord. Chem. Rev.*, 2015, **287**, 15–27.
48 S. Rasul, S. Suzuki, S. Yamaguchi and M. Miyayama, High capacity positive electrodes for secondary Mg-ion batteries, *Electrochim. Acta*, 2012, **82**, 243–249.
49 X. Sun, V. Duffort, B. L. Mehdi, N. D. Browning and L. F. Nazar, Investigation of the Mechanism of Mg Insertion in Birnessite in Nonaqueous and Aqueous Rechargeable Mg-Ion Batteries, *Chem. Mater.*, 2016, **28**, 534–542.
50 N. Wu, Y.-C. Lyu, R.-J. Xiao, X. Yu, Y.-X. Yin, X.-Q. Yang, H. Li, L. Gu and Y.-G. Guo, A highly reversible, low-strain Mg-ion insertion anode material for rechargeable Mg-ion batteries, *NPG Asia Mater.*, 2014, **6**, e120.
51 A. Manthiram, Y. Fu and Y.-S. Su, Challenges and Prospects of Lithium–Sulfur Batteries, *Acc. Chem. Res.*, 2013, **46**, 1125–1134.
52 N. Nakamura, S. Ahn, T. Momma and T. Osaka, Future potential for lithium–sulfur batteries, *J. Power Sources*, 2023, **558**, 232566.
53 Y. Yang, G. Zheng and Y. Cui, Nanostructured sulfur cathodes, *Chem. Soc. Rev.*, 2013, **42**, 3018–3032.
54 J. E. Knoop and S. Ahn, Recent advances in nanomaterials for high-performance Li–S batteries, *J. Energy Chem.*, 2020, **47**, 86–106.
55 B. Zhang, X. Qin, G. R. Li and X. P. Gao, Enhancement of long stability of sulfur cathode by encapsulating sulfur into micropores of carbon spheres, *Energy Environ. Sci.*, 2010, **3**, 1531–1537.
56 Q. Zhao, S. Stalin, C.-Z. Zhao and L. A. Archer, Designing solid-state electrolytes for safe, energy-dense batteries, *Nat. Rev. Mater.*, 2020, **5**, 229–252.
57 J. Wan, J. Xie, D. G. Mackanic, W. Burke, Z. Bao and Y. Cui, Status, promises, and challenges of nanocomposite solid-state electrolytes for safe and high performance lithium batteries, *Mater. Today Nano*, 2018, **4**, 1–16.
58 G. Tan, F. Wu, C. Zhan, J. Wang, D. Mu, J. Lu and K. Amine, Solid-State Li-Ion Batteries Using Fast, Stable, Glassy Nanocomposite Electrolytes for Good Safety and Long Cycle-Life, *Nano Lett.*, 2016, **16**, 1960–1968.
59 Y. Cui, J. Wan, Y. Ye, K. Liu, L.-Y. Chou and Y. Cui, A Fireproof, Lightweight, Polymer–Polymer Solid-State Electrolyte for Safe Lithium Batteries, *Nano Lett.*, 2020, **20**, 1686–1692.

60 A. Manthiram, X. Yu and S. Wang, Lithium battery chemistries enabled by solid-state electrolytes, *Nat. Rev. Mater.*, 2017, **2**, 16103.
61 D. H. S. Tan, A. Banerjee, Z. Chen and Y. S. Meng, From nanoscale interface characterization to sustainable energy storage using all-solid-state batteries, *Nat. Nanotechnol.*, 2020, **15**, 170–180.
62 S. Randau, D. A. Weber, O. Kötz, R. Koerver, P. Braun, A. Weber, E. Ivers-Tiffée, T. Adermann, J. Kulisch, W. G. Zeier, F. H. Richter and J. Janek, Benchmarking the performance of all-solid-state lithium batteries, *Nat. Energy*, 2020, **5**, 259–270.
63 A. Banerjee, X. Wang, C. Fang, E. A. Wu and Y. S. Meng, Interfaces and Interphases in All-Solid-State Batteries with Inorganic Solid Electrolytes, *Chem. Rev.*, 2020, **120**, 6878–6933.
64 Y. Kato, S. Hori, T. Saito, K. Suzuki, M. Hirayama, A. Mitsui, M. Yonemura, H. Iba and R. Kanno, High-power all-solid-state batteries using sulfide superionic conductors, *Nat. Energy*, 2016, **1**, 16030.
65 R. C. Agrawal and G. P. Pandey, Solid polymer electrolytes: materials designing and all-solid-state battery applications: an overview, *J. Phys. D: Appl. Phys.*, 2008, **41**, 223001.
66 R. Koerver, W. Zhang, L. de Biasi, S. Schweidler, A. O. Kondrakov, S. Kolling, T. Brezesinski, P. Hartmann, W. G. Zeier and J. Janek, Chemo-mechanical expansion of lithium electrode materials – on the route to mechanically optimized all-solid-state batteries, *Energy Environ. Sci.*, 2018, **11**, 2142–2158.
67 C. Yu, S. Ganapathy, E. R. H. V. Eck, H. Wang, S. Basak, Z. Li and M. Wagemaker, Accessing the bottleneck in all-solid state batteries, lithium-ion transport over the solid-electrolyte-electrode interface, *Nat. Commun.*, 2017, **8**, 1086.
68 R. Gond, W. van Ekeren, R. Mogensen, A. J. Naylor and R. Younesi, Non-flammable liquid electrolytes for safe batteries, *Mater. Horiz.*, 2021, **8**, 2913–2928.
69 F. Gebert, M. Longhini, F. Conti and A. J. Naylor, An electrochemical evaluation of state-of-the-art non-flammable liquid electrolytes for high-voltage lithium-ion batteries, *J. Power Sources*, 2023, **556**, 232412.
70 H. Sun, G. Zhu, X. Xu, M. Liao, Y.-Y. Li, M. Angell, M. Gu, Y. Zhu, W. H. Hung, J. Li, Y. Kuang, Y. Meng, M.-C. Lin, H. Peng and H. Dai, A safe and non-flammable sodium metal battery based on an ionic liquid electrolyte, *Nat. Commun.*, 2019, **10**, 3302.
71 P. Sun, R. Bisschop, H. Niu and X. Huang, A Review of Battery Fires in Electric Vehicles, *Fire Technol.*, 2020, **56**, 1361–1410.
72 P. Victor Chombo, Y. Laoonual and S. Wongwises, Lessons from the Electric Vehicle Crashworthiness Leading to Battery Fire, *Energies*, 2021, **14**, 4802.
73 M. Held, M. Tuchschmid, M. Zennegg, R. Figi, C. Schreiner, L. D. Mellert, U. Welte, M. Kompatscher, M. Hermann and L. Nachef, Thermal runaway and fire of electric vehicle lithium-ion battery and contamination of infrastructure facility, *Renewable Sustainable Energy Rev.*, 2022, **165**, 112474.
74 Y. Cui, J. Liu, B. Cong, X. Han and S. Yin, Characterization and assessment of fire evolution process of electric vehicles placed in parallel, *Process Saf. Environ. Prot.*, 2022, **166**, 524–534.
75 S. Kang, M. Kwon, J. Yoon Choi and S. Choi, Full-scale fire testing of battery electric vehicles, *Appl. Energy*, 2023, **332**, 120497.
76 A. Chen, C. Qu, Y. Shi and F. Shi, Manufacturing Strategies for Solid Electrolyte in Batteries, *Front. Energy Res.*, 2020, **8**, 571440.
77 R. Murugan, V. Thangadurai and W. Weppner, Fast Lithium Ion Conduction in Garnet-Type $Li_7La_3Zr_2O_{12}$, *Angew. Chem., Int. Ed.*, 2007, **46**, 7778–7781.
78 T. Asano, A. Sakai, S. Ouchi, M. Sakaida, A. Miyazaki and S. Hasegawa, Solid Halide Electrolytes with High Lithium-Ion Conductivity for Application in 4 V Class Bulk-Type All-Solid-State Batteries, *Adv. Mater.*, 2018, **30**, 1803075.
79 K.-H. Park, K. Kaup, A. Assoud, Q. Zhang, X. Wu and L. F. Nazar, High-Voltage Superionic Halide Solid Electrolytes for All-Solid-State Li-Ion Batteries, *ACS Energy Lett.*, 2020, **5**, 533–539.
80 H.-J. Deiseroth, S.-T. Kong, H. Eckert, J. Vannahme, C. Reiner, T. Zaiß and M. Schlosser, Li6PS5X: A Class of Crystalline Li-Rich Solids With an Unusually High Li+ Mobility, *Angew. Chem., Int. Ed.*, 2008, **47**, 755–758.
81 P. Adeli, J. D. Bazak, K. H. Park, I. Kochetkov, A. Huq, G. R. Goward and L. F. Nazar, Boosting Solid-State Diffusivity and Conductivity in Lithium Superionic Argyrodites by Halide Substitution, *Angew. Chem., Int. Ed.*, 2019, **58**, 8681–8686.
82 Y. Li, S. Song, H. Kim, K. Nomoto, H. Kim, X. Sun, S. Hori, K. Suzuki, N. Matsui, M. Hirayama, T. Mizoguchi, T. Saito, T. Kamiyama and R. Kanno, A lithium superionic conductor for millimeter-thick battery electrode, *Science*, 2023, **381**, 50–53.
83 L. Chen, Y. Li, S.-P. Li, L.-Z. Fan, C.-W. Nan and J. B. Goodenough, PEO/garnet composite electrolytes for solid-state lithium batteries: From ''ceramic-in-polymer'' to ''polymer-in-ceramic'', *Nano Energy*, 2018, **46**, 176–184.
84 S. Kim, H. Oguchi, N. Toyama, T. Sato, S. Takagi, T. Otomo, D. Arunkumar, N. Kuwata, J. Kawamura and S.-I. Orimo, A complex hydride lithium superionic conductor for high-energy-density all-solid-state lithium metal batteries, *Nat. Commun.*, 2019, **10**, 1081.
85 S.-K. Jung, H. Gwon, G. Yoon, L. J. Miara, V. Lacivita and J.-S. Kim, Pliable Lithium Superionic Conductor for All-Solid-State Batteries, *ACS Energy Lett.*, 2021, **6**, 2006–2015.
86 M. J. Lee, J. Han, K. Lee, Y. J. Lee, B. G. Kim, K.-N. Jung, B. J. Kim and S. W. Lee, Elastomeric electrolytes for high-energy solid-state lithium batteries, *Nature*, 2022, **601**, 217–222.
87 W. G. Suci, H. K. Aliwarga, Y. R. Azinuddin, R. B. Setyawati, K. N. R. Stulasti and A. Purwanto, Review of various sulfide electrolyte types for solid-state lithium-ion batteries, *Open Eng.*, 2022, **12**, 409–423.
88 H. Gamo, A. Nagai and A. Matsuda, Toward Scalable Liquid-Phase Synthesis of Sulfide Solid Electrolytes for All-Solid-State Batteries, *Batteries*, 2023, **9**, 355.

89 A. Miura, N. C. Rosero-Navarro, A. Sakuda, K. Tadanaga, N. H. H. Phuc, A. Matsuda, N. Machida, A. Hayashi and M. Tatsumisago, Liquid-phase syntheses of sulfide electrolytes for all-solid-state lithium battery, *Nat. Rev. Chem.*, 2019, **3**, 189–198.

90 S. Ohsaki, T. Yano, A. Hatada, H. Nakamura and S. Watano, Size control of sulfide-based solid electrolyte particles through liquid-phase synthesis, *Powder Technol.*, 2021, **387**, 415–420.

91 Y. Huh, H. Gon Lee, C.-M. Cho, J.-W. Park, B. Gon Kim, Y.-J. Lee, H. Park, Y.-C. Ha, J.-H. Choi, J. Yi, S.-M. Lee, J. In Lee and J.-H. Park, Solution-Processed Synthesis of Nano-Sized Argyrodite Solid Electrolytes with Cavitation Effect for High Performance All-Solid-State Lithium-Ion Batteries, *Batteries Supercaps*, 2023, **6**, e202300036.

92 J. E. Lee, K.-H. Park, J. C. Kim, T.-U. Wi, A. R. Ha, Y. B. Song, D. Y. Oh, J. Woo, S. H. Kweon, S. J. Yeom, W. Cho, K. Kim, H.-W. Lee, S. K. Kwak and Y. S. Jung, Universal Solution Synthesis of Sulfide Solid Electrolytes Using Alkahest for All-Solid-State Batteries, *Adv. Mater.*, 2022, **34**, 2200083.

93 Y. Subramanian, R. Rajagopal and K.-S. Ryu, High ionic-conducting Li-argyrodites synthesized using a simple and economic liquid-phase approach and their application in all solid-state-lithium batteries, *Scr. Mater.*, 2021, **204**, 114129.

94 H. Wang, Z. D. Hood, Y. Xia and C. Liang, Fabrication of ultrathin solid electrolyte membranes of β-Li3PS4 nanoflakes by evaporation-induced self-assembly for all-solid-state batteries, *J. Mater. Chem. A*, 2016, **4**, 8091–8096.

95 S. Teragawa, K. Aso, K. Tadanaga, A. Hayashi and M. Tatsumisago, Preparation of Li2S–P2S5 solid electrolyte from N-methylformamide solution and application for all-solid-state lithium battery, *J. Power Sources*, 2014, **248**, 939–942.

96 S. Ito, M. Nakakita, Y. Aihara, T. Uehara and N. Machida, A synthesis of crystalline $Li_7P_3S_{11}$ solid electrolyte from 1,2-dimethoxyethane solvent, *J. Power Sources*, 2014, **271**, 342–345.

97 R. C. Xu, X. H. Xia, Z. J. Yao, X. L. Wang, C. D. Gu and J. P. Tu, Preparation of $Li_7P_3S_{11}$ glass-ceramic electrolyte by dissolution-evaporation method for all-solid-state lithium ion batteries, *Electrochim. Acta*, 2016, **219**, 235–240.

98 H.-D. Lim, X. Yue, X. Xing, V. Petrova, M. Gonzalez, H. Liu and P. Liu, Designing solution chemistries for the low-temperature synthesis of sulfide-based solid electrolytes, *J. Mater. Chem. A*, 2018, **6**, 7370–7374.

99 I.-H. Choi, E. Kim, Y.-S. Jo, J.-W. Hong, J. Sung, J. Seo, B. Gon Kim, J.-H. Park, Y.-J. Lee, Y.-C. Ha, D. Kim, J. Hong Lee and J.-W. Park, Solvent-engineered synthesis of sulfide solid electrolytes for high performance all-solid-state batteries, *J. Ind. Eng. Chem.*, 2023, **121**, 107–113.

100 N. H. H. Phuc, T. Yamamoto, H. Muto and A. Matsuda, Fast synthesis of Li2S–P2S5–LiI solid electrolyte precursors, *Inorg. Chem. Front.*, 2017, **4**, 1660–1664.

101 L. Zhou, K.-H. Park, X. Sun, F. Lalère, T. Adermann, P. Hartmann and L. F. Nazar, Solvent-Engineered Design of Argyrodite Li6PS5X (X = Cl, Br, I) Solid Electrolytes with High Ionic Conductivity, *ACS Energy Lett.*, 2019, **4**, 265–270.

102 F. Tu, Z. Zhao, X. Zhang, Z. Wang, Y. Ma, H. Zhang, D. Song, L. Zhang, Y. Yang and L. Zhu, Low-Cost and Scalable Synthesis of High-Purity Li2S for Sulfide Solid Electrolyte, *ACS Sustainable Chem. Eng.*, 2022, **10**, 15365–15371.

103 M.-J. Kim, I.-H. Choi, S. C. Jo, B. G. Kim, Y.-C. Ha, S.-M. Lee, S. Kang, K.-J. Baeg and J.-W. Park, A Novel Strategy to Overcome the Hurdle for Commercial All-Solid-State Batteries via Low-Cost Synthesis of Sulfide Solid Electrolytes, *Small Methods*, 2021, **5**, 2100793.

104 A. Han, R. Tian, L. Fang, F. Wan, X. Hu, Z. Zhao, F. Tu, D. Song, X. Zhang and Y. Yang, A Low-Cost Liquid-Phase Method of Synthesizing High-Performance Li6PS5Cl Solid-Electrolyte, *ACS Appl. Mater. Interfaces*, 2022, **14**, 30824–30838.

105 K. Wang, Q. Ren, Z. Gu, C. Duan, J. Wang, F. Zhu, Y. Fu, J. Hao, J. Zhu, L. He, C.-W. Wang, Y. Lu, J. Ma and C. Ma, A cost-effective and humidity-tolerant chloride solid electrolyte for lithium batteries, *Nat. Commun.*, 2021, **12**, 4410.

106 Y.-S. Jo, J.-W. Hong, I.-H. Choi, J. Sung, J.-H. Park, H. Park, D. Kim, B. G. Kim, Y.-C. Ha, J. Seo, W.-Y. Chung, K.-J. Baeg and J.-W. Park, Engineering green and sustainable solvents for scalable wet synthesis of sulfide electrolytes in high-energy-density all-solid-state batteries, *Green Chem.*, 2023, **25**, 1473–1487.

107 R. Ye, N. Hamzelui, M. Ihrig, M. Finsterbusch and E. Figgemeier, Water-Based Fabrication of a $Li|Li_7La_3Zr_2O_{12}|-LiFePO_4$ Solid-State Battery—Toward Green Battery Production, *ACS Sustainable Chem. Eng.*, 2022, **10**, 7613–7624.

108 L. Azhari, S. Bong, X. Ma and Y. Wang, Recycling for All Solid-State Lithium-Ion Batteries, *Matter*, 2020, **3**, 1845–1861.

109 Z. Qin, Y. Xie, X. Meng, D. Qian, D. Mao, X. Ma, C. Shan, J. Chen, L. Wan and Y. Huang, Recycling garnet-type electrolyte toward superior cycling performance for solid-state lithium batteries, *Energy Storage Mater.*, 2022, **49**, 360–369.

110 D. H. S. Tan, P. Xu, H. Yang, M.-C. Kim, H. Nguyen, E. A. Wu, J.-M. Doux, A. Banerjee, Y. S. Meng and Z. Chen, Sustainable design of fully recyclable all solid-state batteries, *MRS Energy Sustainability*, 2020, **7**, 23.

111 S. Dasarathan, J. Sung, M. Ali, J.-W. Park and D. Kim, Non-flammable free-standing TiO_2 nanotubular hybrid membrane prepared by a two-step anodization, *Electrochem. Commun.*, 2023, **151**, 107498.

112 S. Liu, L. Zhou, J. Han, K. Wen, S. Guan, C. Xue, Z. Zhang, B. Xu, Y. Lin, Y. Shen, L. Li and C.-W. Nan, Super Long-Cycling All-Solid-State Battery with Thin Li_6PS_5Cl-Based Electrolyte, *Adv. Energy Mater.*, 2022, **12**, 2200660.

113 D. H. S. Tan, A. Banerjee, Z. Deng, E. A. Wu, H. Nguyen, J.-M. Doux, X. Wang, J.-H. Cheng, S. P. Ong, Y. S. Meng and Z. Chen, Enabling Thin and Flexible Solid-State Composite Electrolytes by the Scalable Solution Process, *Adv. Energy Mater.*, 2019, **2**, 6542–6550.

114 S. H. Kang, J. Y. Kim, D. O. Shin, M. J. Lee and Y.-G. Lee, 2D argyrodite LPSCl solid electrolyte for all-solid-state Li-ion battery using reduced graphene oxide template, *Mater. Today Energy*, 2022, **23**, 100913.

115 D. H. Kim, Y.-H. Lee, Y. B. Song, H. Kwak, S.-Y. Lee and Y. S. Jung, Thin and Flexible Solid Electrolyte Membranes with Ultrahigh Thermal Stability Derived from Solution-Processable Li Argyrodites for All-Solid-State Li-Ion Batteries, *ACS Energy Lett.*, 2020, **5**, 718–727.

116 T. Wei, Z.-H. Zhang, Z.-M. Wang, Q. Zhang, Y.-S. Ye, J.-H. Lu, Z. U. Rahman and Z.-W. Zhang, Ultrathin Solid Composite Electrolyte Based on $Li_{6.4}La_3Zr_{1.4}Ta_{0.6}O_{12}$/PVDF-HFP/LiTFSI/Succinonitrile for High-Performance Solid-State Lithium Metal Batteries, *ACS Appl. Energy Mater.*, 2020, **3**, 9428–9435.

117 S. H. Kang, J. Choi, J. Y. Kim, D. O. Shin, Y.-G. Lee and J. Lee, Mechanically Robust Ultrathin Solid Electrolyte Membranes Using a Porous Net Template for All-Solid-State Batteries, *ACS Appl. Mater. Interfaces*, 2023, **15**, 28064–28072.

118 Z. Zhang, L. Wu, D. Zhou, W. Weng and X. Yao, Flexible Sulfide Electrolyte Thin Membrane with Ultrahigh Ionic Conductivity for All-Solid-State Lithium Batteries, *Nano Lett.*, 2021, **21**, 5233–5239.

119 J. Reinacher, S. Berendts and J. Janek, Preparation and electrical properties of garnet-type $Li_6BaLa_2Ta_2O_{12}$ lithium solid electrolyte thin films prepared by pulsed laser deposition, *Solid State Ionics*, 2014, **258**, 1–7.

120 X. Wang and G. Yushin, Chemical vapor deposition and atomic layer deposition for advanced lithium ion batteries and supercapacitors, *Energy Environ. Sci.*, 2015, **8**, 1889–1904.

121 C. Loho, R. Djenadic, M. Bruns, O. Clemens and H. Hahn, Garnet-Type $Li_7La_3Zr_2O_{12}$ Solid Electrolyte Thin Films Grown by CO_2-Laser Assisted CVD for All-Solid-State Batteries, *J. Electrochem. Soc.*, 2017, **164**, A6131.

122 J. Li, Y. Li, S. Zhang, T. Liu, D. Li and L. Ci, In Situ Formed LiI Interfacial Layer for All-Solid-State Lithium Batteries with Li_6PS_5Cl Solid Electrolyte Membranes, *ACS Appl. Mater. Interfaces*, 2022, **14**, 55727–55734.

123 N. Yang, Y. Cui, H. Su, J. Peng, Y. Shi, J. Niu and F. Wang, A Chemically Bonded Ultraconformal Layer between the Elastic Solid Electrolyte and Lithium Anode for High-performance Lithium Metal Batteries, *Angew. Chem., Int. Ed.*, 2023, **62**, e202304339.

124 R. W. Johnson, A. Hultqvist and S. F. Bent, A brief review of atomic layer deposition: from fundamentals to applications, *Mater. Today*, 2014, **17**, 236–246.

125 C.-F. Li, R. Muruganantham, W.-C. Hsu, M. Ihrig, C.-T. Hsieh, C.-C. Wang and W.-R. Liu, Atomic layer deposition of ZnO on $Li_{1.3}Al_{0.3}Ti_{1.7}(PO_4)_3$ enables its application in all solid-state lithium batteries, *J. Taiwan Inst. Chem. Eng.*, 2023, **144**, 104681.

126 B. Wang, J. Liu, M. Norouzi Banis, Q. Sun, Y. Zhao, R. Li, T.-K. Sham and X. Sun, Atomic Layer Deposited Lithium Silicates as Solid-State Electrolytes for All-Solid-State Batteries, *ACS Appl. Mater. Interfaces*, 2017, **9**, 31786–31793.

127 J. Su, T. Tsuruoka, T. Tsujita, Y. Inatomi and K. Terabe, Nitrogen Plasma Enhanced Low Temperature Atomic Layer Deposition of Magnesium Phosphorus Oxynitride (MgPON) Solid-State Electrolytes, *Angew. Chem., Int. Ed.*, 2023, **62**, e202217203.

128 J. Sang, B. Tang, K. Pan, Y.-B. He and Z. Zhou, Current Status and Enhancement Strategies for All-Solid-State Lithium Batteries, *Acc. Mater. Res.*, 2023, **4**, 472–483.

129 F. Hippauf, B. Schumm, S. Doerfler, H. Althues, S. Fujiki, T. Shiratsuchi, T. Tsujimura, Y. Aihara and S. Kaskel, Overcoming binder limitations of sheet-type solid-state cathodes using a solvent-free dry-film approach, *Energy Storage Mater.*, 2019, **21**, 390–398.

130 Y. Zhang, F. Huld, S. Lu, C. Jektvik, F. Lou and Z. Yu, Revisiting Polytetrafluorethylene Binder for Solvent-Free Lithium-Ion Battery Anode Fabrication, *Batteries*, 2022, **8**, 57.

131 W. Yan, Z. Mu, Z. Wang, Y. Huang, D. Wu, P. Lu, J. Lu, J. Xu, Y. Wu, T. Ma, M. Yang, X. Zhu, Y. Xia, S. Shi, L. Chen, H. Li and F. Wu, Hard-carbon-stabilized Li–Si anodes for high-performance all-solid-state Li-ion batteries, *Nat. Energy*, 2023, **8**, 800–813.

132 B. Ludwig, Z. Zheng, W. Shou, Y. Wang and H. Pan, Solvent-Free Manufacturing of Electrodes for Lithium-ion Batteries, *Sci. Rep.*, 2016, **6**, 23150.

133 D. Y. Oh, K. T. Kim, S. H. Jung, D. H. Kim, S. Jun, S. Jeoung, H. R. Moon and Y. S. Jung, Tactical hybrids of Li + -conductive dry polymer electrolytes with sulfide solid electrolytes: Toward practical all-solid-state batteries with wider temperature operability, *Mater. Today*, 2022, **53**, 7–15.

134 M. Yamamoto, Y. Terauchi, A. Sakuda and M. Takahashi, Binder-free sheet-type all-solid-state batteries with enhanced rate capabilities and high energy densities, *Sci. Rep.*, 2018, **8**, 1212.

135 K. T. Kim, T. Y. Kwon, Y. B. Song, S.-M. Kim, S. C. Byun, H.-S. Min, S. H. Kim and Y. S. Jung, Wet-slurry fabrication using PVdF-HFP binder with sulfide electrolytes via synergetic cosolvent approach for all-solid-state batteries, *Chem. Eng. J.*, 2022, **450**, 138047.

136 T. Y. Kwon, K. T. Kim, D. Y. Oh, Y. B. Song, S. Jun and Y. S. Jung, Three-dimensional networking binders prepared in situ during wet-slurry process for all-solid-state batteries operating under low external pressure, *Energy Storage Mater.*, 2022, **49**, 219–226.

137 K. H. Park, D. Y. Oh, Y. E. Choi, Y. J. Nam, L. Han, J.-Y. Kim, H. Xin, F. Lin, S. M. Oh and Y. S. Jung, Solution-Processable Glass LiI-Li4SnS4 Superionic Conductors for All-Solid-State Li-Ion Batteries, *Adv. Mater.*, 2016, **28**, 1874–1883.

138 D. Y. Oh, D. H. Kim, S. H. Jung, J.-G. Han, N.-S. Choi and Y. S. Jung, Single-step wet-chemical fabrication of sheet-type electrodes from solid-electrolyte precursors for all-solid-state lithium-ion batteries, *J. Mater. Chem. A*, 2017, **5**, 20771–20779.

139 D. H. Kim, D. Y. Oh, K. H. Park, Y. E. Choi, Y. J. Nam, H. A. Lee, S.-M. Lee and Y. S. Jung, Infiltration of Solution-Processable Solid Electrolytes into Conventional Li-Ion-Battery Electrodes for All-Solid-State Li-Ion Batteries, *Nano Lett.*, 2017, **17**, 3013–3020.

140 D. H. Kim, H. A. Lee, Y. B. Song, J. W. Park, S.-M. Lee and Y. S. Jung, Sheet-type Li6PS5Cl-infiltrated Si anodes fabricated by solution process for all-solid-state lithium-ion batteries, *J. Power Sources*, 2019, **426**, 143–150.

141 Y. B. Song, D. H. Kim, H. Kwak, D. Han, S. Kang, J. H. Lee, S.-M. Bak, K.-W. Nam, H.-W. Lee and Y. S. Jung, Tailoring Solution-Processable Li Argyrodites $Li_{6+x}P_{1-x}M_xS5I$ (M = Ge, Sn) and Their Microstructural Evolution Revealed by Cryo-TEM for All-Solid-State Batteries, *Nano Lett.*, 2020, **20**, 4337–4345.

142 M.-J. Kim, J.-W. Park, B. G. Kim, Y.-J. Lee, Y.-C. Ha, S.-M. Lee and K.-J. Baeg, Facile fabrication of solution-processed solid-electrolytes for high-energy-density all-solid-state-batteries by enhanced interfacial contact, *Sci. Rep.*, 2020, **10**, 11923.

143 A. Banerjee, K. H. Park, J. W. Heo, Y. J. Nam, C. K. Moon, S. M. Oh, S.-T. Hong and Y. S. Jung, Na3SbS4: A Solution Processable Sodium Superionic Conductor for All-Solid-State Sodium-Ion Batteries, *Angew. Chem., Int. Ed.*, 2016, **55**, 9634–9638.

144 L. Duchêne, D. H. Kim, Y. B. Song, S. Jun, R. Moury, A. Remhof, H. Hagemann, Y. S. Jung and C. Battaglia, Crystallization of closo-borate electrolytes from solution enabling infiltration into slurry-casted porous electrodes for all-solid-state batteries, *Energy Storage Mater.*, 2020, **26**, 543–549.

145 T. Liu, H. Hu, X. Ding, H. Yuan, C. Jin, J. Nai, Y. Liu, Y. Wang, Y. Wan and X. Tao, 12 years roadmap of the sulfur cathode for lithium sulfur batteries (2009–2020), *Energy Storage Mater.*, 2020, **30**, 346–366.

146 H. Li, Y. Li and L. Zhang, Designing principles of advanced sulfur cathodes toward practical lithium–sulfur batteries, *SusMat*, 2022, **2**, 34–64.

147 B. He, Z. Rao, Z. Cheng, D. Liu, D. He, J. Chen, Z. Miao, L. Yuan, Z. Li and Y. Huang, Rationally Design a Sulfur Cathode with Solid-Phase Conversion Mechanism for High Cycle-Stable Li–S Batteries, *Adv. Energy Mater.*, 2021, **11**, 2003690.

148 J. Yang, G. Liu, M. Avdeev, H. Wan, F. Han, L. Shen, Z. Zou, S. Shi, Y.-S. Hu, C. Wang and X. Yao, Ultrastable All-Solid-State Sodium Rechargeable Batteries, *ACS Energy Lett.*, 2020, **5**, 2835–2841.

149 S. Gandi, V. S. Chidambara Swamy Vaddadi, S. S. Sripada Panda, N. K. Goona, S. R. Parne, M. Lakavat and A. Bhaumik, Recent progress in the development of glass and glass-ceramic cathode/solid electrolyte materials for next-generation high capacity all-solid-state sodium-ion batteries: A review, *J. Power Sources*, 2022, **521**, 230930.

150 Y. Yao, Z. Wei, H. Wang, H. Huang, Y. Jiang, X. Wu, X. Yao, Z.-S. Wu and Y. Yu, Toward High Energy Density All Solid-State Sodium Batteries with Excellent Flexibility, *Adv. Energy Mater.*, 2020, **10**, 1903698.

151 Y. Yan, J. B. Grinderslev, M. Jrgensen, L. N. Skov, J. R. Skibsted and T. R. Jensen, Ammine Magnesium Borohydride Nanocomposites for All-Solid-State Magnesium Batteries, *Adv. Energy Mater.*, 2020, **3**, 9264–9270.

152 M. B. Amdisen, J. B. Grinderslev, L. N. Skov and T. R. Jensen, Methylamine Magnesium Borohydrides as Electrolytes for All-Solid-State Magnesium Batteries, *Chem. Mater.*, 2023, **35**, 1440–1448.

153 L. N. Skov, J. B. Grinderslev and T. R. Jensen, Layered Titanium Sulfide Cathode for All-Solid-State Magnesium Batteries, *Batteries Supercaps*, 2023, **6**, e202300185.

154 H. Pan, Z. Cheng, P. He and H. Zhou, A Review of Solid-State Lithium–Sulfur Battery: Ion Transport and Polysulfide Chemistry, *Energy Fuels*, 2020, **34**, 11942–11961.

155 H. Wan, S. Liu, T. Deng, J. Xu, J. Zhang, X. He, X. Ji, X. Yao and C. Wang, Bifunctional Interphase-Enabled $Li_{10}GeP2S_{12}$ Electrolytes for Lithium–Sulfur Battery, *ACS Energy Lett.*, 2021, **6**, 862–868.

156 J. Yi, L. Chen, Y. Liu, H. Geng and L.-Z. Fan, High Capacity and Superior Cyclic Performances of All-Solid-State Lithium–Sulfur Batteries Enabled by a High-Conductivity $Li_{10}SnP_2S_{12}$ Solid Electrolyte, *ACS Appl. Mater. Interfaces*, 2019, **11**, 36774–36781.

157 S. A. Pervez, B. P. Vinayan, M. A. Cambaz, G. Melinte, T. Diemant, T. Braun, G. Karkera, R. J. Behm and M. Fichtner, Electrochemical and compositional characterization of solid interphase layers in an interface-modified solid-state Li–sulfur battery, *J. Mater. Chem. A*, 2020, **8**, 16451–16462.

158 S.-H. Kim, J.-H. Kim, S.-J. Cho and S.-Y. Lee, All-Solid-State Printed Bipolar Li–S Batteries, *Adv. Energy Mater.*, 2019, **9**, 1901841.

159 M. Li, J. E. Frerichs, M. Kolek, W. Sun, D. Zhou, C. J. Huang, B. J. Hwang, M. R. Hansen, M. Winter and P. Bieker, Solid-State Lithium–Sulfur Battery Enabled by Thio-LiSICON/Polymer Composite Electrolyte and Sulfurized Polyacrylonitrile Cathode, *Adv. Funct. Mater.*, 2020, **30**, 1910123.

160 Q. Liu, Z. Hu, W. Li, C. Zou, H. Jin, S. Wang, S. Chou and S.-X. Dou, Sodium transition metal oxides: the preferred cathode choice for future sodium-ion batteries?, *Energy Environ. Sci.*, 2021, **14**, 158–179.

161 J. Xiao, X. Li, K. Tang, D. Wang, M. Long, H. Gao, W. Chen, C. Liu, H. Liu and G. Wang, Recent progress of emerging cathode materials for sodium ion batteries, *Mater. Chem. Front.*, 2021, **5**, 3735–3764.

162 Y.-B. Niu, Y.-J. Guo, Y.-X. Yin, S.-Y. Zhang, T. Wang, P. Wang, S. Xin and Y.-G. Guo, High-Efficiency Cathode Sodium Compensation for Sodium-Ion Batteries, *Adv. Mater.*, 2020, **32**, 2001419.

163 Q. Liu, Z. Hu, M. Chen, C. Zou, H. Jin, S. Wang, S.-L. Chou, Y. Liu and S.-X. Dou, The Cathode Choice for Commercialization of Sodium-Ion Batteries: Layered Transition Metal Oxides versus Prussian Blue Analogs, *Adv. Funct. Mater.*, 2020, **30**, 1909530.

164 A. Rudola, A. J. R. Rennie, R. Heap, S. S. Meysami, A. Lowbridge, F. Mazzali, R. Sayers, C. J. Wright and J. Barker, Commercialisation of high energy density sodium-ion batteries: Faradion's journey and outlook, *J. Mater. Chem. A*, 2021, **9**, 8279–8302.

165 C. Zhao, L. Liu, X. Qi, Y. Lu, F. Wu, J. Zhao, Y. Yu, Y.-S. Hu and L. Chen, Solid-State Sodium Batteries, *Adv. Energy Mater.*, 2018, **8**, 1703012.

166 E. Matios, H. Wang, C. Wang, X. Hu, X. Lu, J. Luo and W. Li, Graphene Regulated Ceramic Electrolyte for Solid-State Sodium Metal Battery with Superior Electrochemical Stability, *ACS Appl. Mater. Interfaces*, 2019, **11**, 5064–5072.

167 C.-D. Zhao, J.-Z. Guo, Z.-Y. Gu, X.-T. Wang, X.-X. Zhao, W.-H. Li, H.-Y. Yu and X.-L. Wu, Flexible quasi-solid-state sodium-ion full battery with ultralong cycle life, high energy density and high-rate capability, *Nano Res.*, 2022, **15**, 925–932.

168 M. Rashad, M. Asif, Y. Wang, Z. He and I. Ahmed, Recent advances in electrolytes and cathode materials for magnesium and hybrid-ion batteries, *Energy Storage Mater.*, 2020, **25**, 342–375.

169 P. Wang, J. Trück, S. Niesen, J. Kappler, K. Küster, U. Starke, F. Ziegler, A. Hintennach and M. R. Buchmeiser, High-Performance Magnesium-Sulfur Batteries Based on a Sulfurated Poly(acrylonitrile) Cathode, a Borohydride Electrolyte, and a High-Surface Area Magnesium Anode, *Batteries Supercaps*, 2020, **3**, 1239–1247.

170 C. Zuo, W. Tang, B. Lan, F. Xiong, H. Tang, S. Dong, W. Zhang, C. Tang, J. Li, Y. Ruan, S. Xi, Q. An and P. Luo, Unexpected discovery of magnesium-vanadium spinel oxide containing extractable Mg^{2+} as a high-capacity cathode material for magnesium ion batteries, *Chem. Eng. J.*, 2021, **405**, 127005.

171 J. Du, A. Zhang, Z. Guo, M. Yang, M. Li and S. Xiong, Atomistic Determination of Anisotropic Surface Energy-Associated Growth Patterns of Magnesium Alloy Dendrites, *ACS Omega*, 2017, **2**, 8803–8809.

172 A. Du, H. Zhang, Z. Zhang, J. Zhao, Z. Cui, Y. Zhao, S. Dong, L. Wang, X. Zhou and G. Cui, A Crosslinked Polytetrahydrofuran-Borate-Based Polymer Electrolyte Enabling Wide-Working-Temperature-Range Rechargeable Magnesium Batteries, *Adv. Mater.*, 2019, **31**, 1805930.

173 K. W. Leong, W. Pan, X. Yi, S. Luo, X. Zhao, Y. Zhang, Y. Wang, J. Mao, Y. Chen, J. Xuan, H. Wang and D. Y. C. Leung, Next-generation magnesium-ion batteries: The quasi-solid-state approach to multivalent metal ion storage, *Sci. Adv.*, 2023, **9**, eadh1181.

174 Y.-G. Lee, S. Fujiki, C. Jung, N. Suzuki, N. Yashiro, R. Omoda, D.-S. Ko, T. Shiratsuchi, T. Sugimoto, S. Ryu, J. H. Ku, T. Watanabe, Y. Park, Y. Aihara, D. Im and I. T. Han, High-energy long-cycling all-solid-state lithium metal batteries enabled by silver–carbon composite anodes, *Nat. Energy*, 2020, **5**, 299–308.

175 S. W. Park, H. J. Choi, Y. Yoo, H.-D. Lim, J.-W. Park, Y.-J. Lee, Y.-C. Ha, S.-M. Lee and B. G. Kim, Stable Cycling of All-Solid-State Batteries with Sacrificial Cathode and Lithium-Free Indium Layer, *Adv. Funct. Mater.*, 2022, **32**, 2108203.

176 I. Na, H. Kim, S. Kunze, C. Nam, S. Jo, H. Choi, S. Oh, E. Choi, Y. B. Song, Y. S. Jung, Y. S. Lee and J. Lim, Monolithic 100% Silicon Wafer Anode for All-Solid-State Batteries Achieving High Areal Capacity at Room Temperature, *ACS Energy Lett.*, 2023, **8**, 1936–1943.